

# **A Directional MAC Protocol for MANET**

Kun Liu

A Thesis

in

The Department

of

Electrical and Computer Engineering

Presented in Partial Fulfillment of the Requirements

for the Degree of Master of Applied Science

Concordia University

Montreal, Quebec, Canada

September 2006

©Kun Liu, 2006



Library and  
Archives Canada

Bibliothèque et  
Archives Canada

Published Heritage  
Branch

Direction du  
Patrimoine de l'édition

395 Wellington Street  
Ottawa ON K1A 0N4  
Canada

395, rue Wellington  
Ottawa ON K1A 0N4  
Canada

*Your file* *Votre référence*  
*ISBN: 978-0-494-28920-4*  
*Our file* *Notre référence*  
*ISBN: 978-0-494-28920-4*

**NOTICE:**

The author has granted a non-exclusive license allowing Library and Archives Canada to reproduce, publish, archive, preserve, conserve, communicate to the public by telecommunication or on the Internet, loan, distribute and sell theses worldwide, for commercial or non-commercial purposes, in microform, paper, electronic and/or any other formats.

The author retains copyright ownership and moral rights in this thesis. Neither the thesis nor substantial extracts from it may be printed or otherwise reproduced without the author's permission.

**AVIS:**

L'auteur a accordé une licence non exclusive permettant à la Bibliothèque et Archives Canada de reproduire, publier, archiver, sauvegarder, conserver, transmettre au public par télécommunication ou par l'Internet, prêter, distribuer et vendre des thèses partout dans le monde, à des fins commerciales ou autres, sur support microforme, papier, électronique et/ou autres formats.

L'auteur conserve la propriété du droit d'auteur et des droits moraux qui protègent cette thèse. Ni la thèse ni des extraits substantiels de celle-ci ne doivent être imprimés ou autrement reproduits sans son autorisation.

---

In compliance with the Canadian Privacy Act some supporting forms may have been removed from this thesis.

Conformément à la loi canadienne sur la protection de la vie privée, quelques formulaires secondaires ont été enlevés de cette thèse.

While these forms may be included in the document page count, their removal does not represent any loss of content from the thesis.

Bien que ces formulaires aient inclus dans la pagination, il n'y aura aucun contenu manquant.

  
**Canada**

# Abstract

## A Directional MAC Protocol for MANET

Kun Liu

In a typical mobile ad hoc network (MANET), all nodes contend for a single channel access using carrier sense multiple access with collision avoidance (CSMA/CA). Thus, a fundamental limitation of MANET is that, as the number of nodes increases, the performance of the system will dramatically degrade due to the large number of collisions. This, in turn, results in an overall low system throughput.

Several researchers have focused on the potential throughput gains achieved using directional antennas in ad hoc networks. When compared to omnidirectional antennas, directional antennas are more attractive option in terms of power and bandwidth efficiency. On the other hand, when used in ad hoc networks, directional MAC (DMAC) protocols usually require all nodes, or part of nodes, to be aware of their exact locations. The location information is typically provided to the DMAC protocol from upper network layers, for example, by using a Global Positioning System (GPS). Other problems that face these DMAC protocols are the deafness problem and the hidden terminal problem.

Solving these problems is at the core of designing any DMAC protocol. At the same time, DMC protocols should not sacrifice channel bandwidth to deal with these problems.

In this thesis, we propose an efficient 2-channel 2-mode DMAC protocol. In particular, our protocol employs two frequency division multiplexed channels: Channel

one is used for omni mode packets transmission and channel two is used for directional mode packets transmission. Estimation of Signal Parameter via Rotational Invariance Technique (ESPRIT) is used for direction of arrival (DOA) estimation. By avoiding the reliance on GPS for obtaining the position information, our protocol is also suitable for indoor environments.

Under different operating conditions and channel models, our simulation results clearly show the improved throughput of our protocol compared to IEEE 802.11.

# Acknowledgments

First of all, I would like to express my gratitude to my supervisors, Dr. Amr Youssef and Dr. Walaa Hamouda. Their suggestions and guidance are always helpful and insightful. Their scientific attitude and enthusiasm to academic research work will always remain as my model.

In addition, I must acknowledge the tremendous support and encouragement of my friends and lab mates: Ren Wang, Pang Hong, Mohammad Faisal Uddin, Yuxin Pan and Zhao Yin. I cannot thank them enough for their unvarying assistance. It is my great honor to work and study with them.

Finally, and most importantly, I have to extend heartfelt thanks to my parents Yanfu Liu and Xuemin Sun for their unwavering support and unceasing encouragement throughout these many years. Words simply cannot convey how appreciative and thankful I am for having such a selfless, generous parents, not just during the time of preparing this thesis, but throughout my whole life. It is to them that I dedicate this work, with my love and deepest thanks.

# Table of Contents

<b>TABLE OF CONTENTS</b> .....	<b>VI</b>
<b>LIST OF FIGURES</b> .....	<b>VIII</b>
<b>LIST OF NOTATIONS</b> .....	<b>XI</b>
<b>CHAPTER 1</b> .....	<b>1</b>
<b>INTRODUCTION</b> .....	<b>1</b>
1.1 MOTIVATION .....	1
1.2 PREVIOUS WORKS .....	3
1.3 OUTLINE OF THE THESIS .....	6
<b>CHAPTER 2</b> .....	<b>7</b>
<b>BACKGROUND</b> .....	<b>7</b>
2.1 INTRODUCTION .....	7
2.2 IEEE 802.11 .....	7
2.2.1 <i>The IEEE 802.11 standard</i> .....	7
2.2.2 <i>Architecture of the IEEE 802.11 standard</i> .....	8
2.2.3 <i>Frames Structure of the IEEE 802.11</i> .....	13
2.2.4 <i>MAC layer of IEEE 802.11</i> .....	15
2.2.4.1 Distributed Coordination Function (DCF).....	15
2.2.4.2 Point Coordination Function (PCF).....	18
2.2.5 <i>Physical Layer</i> .....	19
2.2.5.1 Frequency hopping spread spectrum .....	20
2.2.5.2 Direct sequence spread spectrum.....	20
2.2.5.3 Infrared.....	20
2.3 ADAPTIVE ANTENNAS .....	21
2.3.1 <i>Uniformly Spaced Linear Antenna Array</i> .....	21
2.3.2 <i>Beamforming of Adaptive Antenna</i> .....	25
2.3.3 <i>Adaptive Algorithm</i> .....	31
2.3.3.1 Least Mean Squares.....	32
2.3.3.2 Recursive least squares (RLS) algorithm.....	33
2.3.3.3 Constant modulus algorithm (CMA).....	33
2.4 DIRECTION OF ARRIVAL (DOA) ESTIMATION ALGORITHMS .....	33
2.4.1 <i>Data Model of ESPRIT</i> .....	34
2.5 SUMMARY .....	38
<b>CHAPTER 3</b> .....	<b>39</b>
<b>DOA ESTIMATION</b> .....	<b>39</b>
3.1 INTRODUCTION .....	39
3.2 EFFECT OF GPS POSITION ESTIMATION ERROR.....	39
3.3 EFFECT OF INACCURATE GPS POSITION ESTIMATION.....	41
3.4 ACCURACY OF THE ESPRIT ESTIMATION ALGORITHM.....	45

3.5 SUMMARY .....	49
<b>CHAPTER 4.....</b>	<b>50</b>
<b>PROTOCOL DESCRIPTION .....</b>	<b>50</b>
4.1 INTRODUCTION .....	50
4.2 PROTOCOL DESCRIPTION.....	50
4.3 DETERMINING THE NUMBER OF ANTENNA ELEMENTS .....	63
4.4 SUMMARY .....	67
<b>CHAPTER 5.....</b>	<b>68</b>
<b>SIMULATION RESULTS .....</b>	<b>68</b>
5.1 INTRODUCTION .....	68
5.2 SYSTEM MODEL .....	68
5.2.1 <i>Topology and Parameters</i> .....	68
5.2.2 <i>Communication Channels</i> .....	70
5.3 SYSTEM PERFORMANCE EVALUATION.....	73
5.3.1 <i>System Performance under Different System Loads</i> .....	74
5.3.2 <i>System Performance under Different SNR</i> .....	75
5.3.3 <i>System Performance under Different NOE</i> .....	77
5.3.4 <i>Number of users</i> .....	78
5.4 SUMMARY .....	80
<b>CHAPTER 6.....</b>	<b>81</b>
<b>CONCLUSIONS AND FUTURE WORK .....</b>	<b>81</b>
6.1 CONCLUSIONS .....	81
6.2 FUTURE WORKS .....	82
<b>REFERENCES.....</b>	<b>83</b>

# List of Figures

Figure 2.1 IEEE 802.11 standards mapped to the OSI reference model. ....	8
Figure 2.2 Independent Basic Service Set. ....	10
Figure 2.3 Infrastructure Basic Service Set. ....	11
Figure 2.4 Extended Service Set. ....	12
Figure 2.5 MAC Frame Format. ....	13
Figure 2.6 Frame Control Field. ....	14
Figure 2.7 IEEE 802.11 MAC architecture. ....	15
Figure 2.8 Basic CSMA/CA operations. ....	16
Figure 2.9 Timing diagram for a transmission process. ....	18
Figure 2.10 Point coordination frame transfer. ....	19
Figure 2.11 An M-element uniformly spaced linear array. ....	22
Figure 2.12 A simple narrowband adaptive array system. ....	26
Figure 2.13 An example where desired DOA=125 deg. ....	29
Figure 2.14 Transmitter's beampattern, NOE=5, $\lambda/2$ spacing between antennas, desired DOA=125 deg. ....	29
Figure 2.15 An example, desired DOA=125 deg, undesired DOA=30 deg. ....	30
Figure 2.16 Transmitter's beampattern, NOE=5, $\lambda/2$ spacing between antennas, desired DOA=125 deg, undesired DOA = 30 deg. ....	30
Figure 3.1 Beampattern of Directional Antenna, NOE=3. ....	40
Figure 3.2 Average throughput for different NOE versus DOA Error (uniform distribution) in AWGN channel, (10 nodes, 30 random topologies), SNR=20dB. ....	42
Figure 3.3 Average throughput for different NOE versus DOA Error (Gaussian distribution) in AWGN channel, (10 stations, 30 random topologies), SNR=20dB. .	43
Figure 3.4 Average throughput for different NOE versus DOA Error (uniform distribution) in AWGN channel, (30 stations, 30 random topologies), SNR=20dB. .	44
Figure 3.5 Average throughput at different NOE versus DOA Error (Gaussian distribution) in AWGN channel, (30 stations, 30 random topologies), SNR=20dB. .	45

Figure 3.6 The effect of SNR versus estimated mean error (SOI=30 degree, NOS=100, $d = \lambda/2$ ).....	46
Figure 3.7 The effect of number of mobile user versus estimated mean error (SOI=30 degree, SNR=20dB, NOS=100, $d = \lambda/2$ ).....	47
Figure 3.8 Number of samples versus estimated mean error (SOI=30 degree, SNR=20dB, $d = \lambda/2$ ).....	48
Figure 3.9 The direction of arrival versus the estimated mean error (SOI=30 degree, SNR=20dB, NOS=100, $d = \lambda/2$ ).....	49
Figure 4.1 An example of the function of the DNAV table.....	51
Figure 4.2 6-node scenario.....	52
Figure 4.3 RTS transmission stage.....	53
Figure 4.4 CTS transmission stage.....	54
Figure 4.5 The blocked direction in the DNAV table.....	56
Figure 4.6 DATA transmission stage.....	57
Figure 4.7 ACK transmission stage.....	58
Figure 4.8 Antenna beamforming for an ongoing transmission (Shadow part is the radio range of the directional antenna).....	59
Figure 4.9 Transmission process for the new MAC protocol.....	60
Figure 4.10 Timing diagram for a 4-station scenario.....	62
Figure 4.11 Illustration of simultaneous estimated signals (step 1).....	64
Figure 4.12 Illustration of simultaneous estimated signals (step 2).....	65
Figure 4.13 Illustration of simultaneous estimated signals (step 3).....	65
Figure 4.14 Illustration of simultaneous estimated signals (step 4).....	66
Figure 4.15 Illustration of simultaneous estimated signals (step 5).....	67
Figure 5.1 Snapshot of a 10-station scenario with random configuration.....	69
Figure 5.2 QPSK signal BER for different channel conditions.....	72
Figure 5.3 Average throughput in AWGN channel (10 mobile nodes and 30 random topologies), SNR = 20dB, NOE= 6 (not applied to IEEE 802.11).....	74

Figure 5.4 Average throughput in AWGN and Ricean (K=6) fading channels (10 mobile nodes and 30 random topologies), Load_per_node=1Mbps, NOE= 6 (not applied to IEEE 802.11).....	76
Figure 5.5 Average throughput in Ricean (K=6) fading channel (10 mobile nodes and 30 random topologies), SNR=30dB.....	77
Figure 5.6 Average throughput in AWGN channel (30 mobile nodes and 30 random topologies), Load_per_node=1Mbps, NOE= 6 (not applied to IEEE 802.11). .....	78
Figure 5.7 Average throughput in AWGN channel (30 mobile nodes and 30 random topologies), SNR = 20dB, NOE = 6 (not applied to IEEE 802.11). .....	79

# List of Notations

ACK	Acknowledgment
AP	Access point
AWGN	Additive white Gaussian noise
BER	Bit error rate
BSS	Basic service set
CFP	Contention-free period
CP	Contention period
CSMA/CA	Carrier sense multiple access with collision avoidance
CSMA/CD	Carrier sense multiple access with collision detection
CTS	Clear to send
DCF	Distribution coordination function
DCTS	Directional CTS
DIFS	Distributed coordination function interframe space
DNAV	Directional network allocation vector
DOA	Direction of arrival
DS	Distribution system
DSSS	Directional sequence spread spectrum
ESS	Extended service set
FHSS	Frequency hopping spread spectrum
GPS	Global positioning system

IBSS	Independent basic service set
IFS	Interframe space
IR	Infrared
LLC	Logical link control
MAC	Medium access control
MPDU	MAC protocol data unit
NAV	Network allocation vector
NOE	Number of elements
NOS	Number of samples
ONAV	Omni-directional network allocation vector
OCTS	Omnidirectional CTS
PHY	Physical layer
PIFS	Point coordination function IFS
RTS	Request to send
SIFS	Short IFS
SNR	Signal to noise ratio
SOI	Signal of intention
STA	Wireless LAN station
ULA	Uniform linear array
WLAN	Wireless LAN

# Chapter 1

## Introduction

### **1.1 Motivation**

An ad hoc network is a collection of, possibly mobile, devices or nodes that are able to establish wireless communications with each other without any pre-existing infrastructure. For such networks, the network control is distributed among the mobile nodes, i.e. no control center or base station is needed. Thus an ad hoc network can be described as a self-organizing and self-configuring multihop wireless network. In Ad hoc networks, each node functions not only as a host but also as a router that maintains routing paths and relays data packets for other nodes in the network that may not be within the direct wireless transmission range. Applications of ad hoc networks include emergency search-and-rescue field, battlefield, and meetings or conventions where people wish to quickly share information.

Normally, all ad hoc nodes are assumed to have only omnidirectional antennas and many existing ad hoc MAC protocols are designed based on this assumption. The main drawback of using omnidirectional antennas is that the electromagnetic energy of the

signal is spread over all directions around the transmitter, while only a small portion of it is received by the intended receiver.

Directional antennas have been proposed as a method to solve this energy/bandwidth waste problem and hence improve the capacity of ad hoc networks. Many works have already focused on how to utilize the benefits of directional antennas in ad hoc MAC protocols. The most important feature of directional antennas is due its capability to cancel co-channel interference. Thus, using directional antennas allows multiple transmissions to co-exist in the same neighborhood. Due to this characteristic, directional antennas constitute an attractive component for all wireless applications.

Besides the device portability factor, some problems may arise when directional antennas are used. These include: deafness, hidden terminal problem and location awareness. The deafness and hidden terminal problems are studied extensively in [11]. The location awareness is a natural problem since the transmitter must know the position or direction of the receiver (i.e., to focus the main lobe on the appropriate direction). To solve the above problems, the majority of directional MAC (DMAC) protocols need to obtain the position information and exchange this information by some proposed frames. Several DMAC protocols (e.g., [10], [15]) assume that all nodes are equipped with a global positioning system (GPS) to be able to determine the position information of the intended user. While the cost of GPS hardware is getting lower, GPS typically requires a line of sight in order to avoid the large signal attenuation and hence is not suitable for indoor applications. Another practical problem that is also ignored by most of the previously proposed GPS-based DMAC protocols is the inaccuracy associated with the GPS position estimation. As indicated by our simulation results, the performance of these

DMAC protocols suffers a large degradation under imperfect position estimation. Moreover, as the position estimation error increases, the system throughput dramatically degrades when using a large number of antenna elements (as will be discussed in chapter 3).

In this thesis, we propose a 2-channel 2-mode DMAC protocol that achieves a large throughput gain relative to other DMAC protocols [10]-[15]. Estimation of signal parameter via rotational invariance technique (ESPRIT) is used for direction of arrival (DOA) estimation.

By employing directional antennas, not only to transmit data frames but also as a tool to estimate the signal DOA, the position estimation is achieved at no additional hardware cost. Moreover, by avoiding the reliance on GPS for obtaining the position information, our protocol is also suitable for indoor environments. By varying the ESPRIT parameters and the number of antenna elements, we are also able to avoid any system capacity degradation caused by inaccurate DOA estimation.

## **1.2 Previous works**

The distributed coordination function (DCF) of the MAC layer protocol defined in the IEEE 802.11 standard is usually used in ad hoc networks [4], [5]. Using Carrier sense multiple access with collision avoidance (CSMA/CA), all nodes in an ad hoc network contend for a single channel access. Therefore, when the number of nodes increases, the performance of the system will dramatically degrade due to the large number of collisions. This, in turn, results in an overall low system throughput.

Recent works on improving the throughput of ad hoc networks have focused on Frequency Division Multiple Access (FDMA) techniques as in [6]-[9]. For instance, the authors in [7] proposed multiple channels MAC protocol based on omnidirectional antennas. In this protocol, ad hoc stations are able to select one channel by checking the status of the  $N$  available channels.

In [6], a similar approach was used to divide the available bandwidth into a number of non overlapping frequency channels. All the above works were aimed at improving the throughput using multiple frequency channels based on a single antenna transmission/reception (i.e., no spatial gain).

Given the most popular bands for the IEEE 802.11 standard being at 2.4 GHz and 5.2 GHz bands, the IEEE 802.11b standard suggests that the frequency distance between two center frequencies of two adjacent channels should be at least 25 MHz far.

As opposed to FDMA based techniques, a more efficient approach to improve the overall system throughput is through the use of directional antennas [10]-[14]. In this approach, all ad hoc nodes are equipped with multiple antennas to facilitate an effective use of the spatial channel among users. Recently many works have focused on the potential gains achieved using directional antennas in ad hoc networks. Among these works, is the proposal of Ko *et al.* [14] where two MAC schemes were proposed: one uses directional request-to-send (DRTS); the other uses both DRTS and omnidirectional RTS (ORTS). Also, Choudhury *et al.* [11] proposed two MAC schemes: (i) a Directional MAC (DMAC) and (ii) Multi-Hop RTS MAC (MMAC). Based on the performance results presented in [11], the authors showed that both DMAC and MMAC perform better than the IEEE 802.11. To solve the out-of-range problem in ad hoc networks, Takata *et al.*

in [12] and [13] proposed what is called a Smart antennas Based Wider-range Access MAC Protocol (SWAMP). This protocol consists of two main modes: omnidirectional transmission range communications mode (OC-mode) and extend omnidirectional transmission range communications mode (ECmode). Also within their work, the authors conducted a performance comparison where they have shown that the simple EC-mode performs as efficient as the MMAC.

A general problem in the MAC schemes presented in [11]-[14] is the hidden terminal problem, resulting from the transmission of directional request-to-send and directional clear-to-send directional (DCTS). This problem arises when the use of directional RTS and directional CTS lead to situations where some stations (i.e., the ones that did not receive DRTS and DCTS) may not notice the ongoing transmissions even if these stations are within the transmission range of the active ones. Furthermore, the transmitted beam patterns in [11]-[14] are only determined by the position of the destination station, without taking the interfering signals into consideration.

Other related works on the implementation of MAC protocols in multiple antenna systems include the work in [16]-[18]. Similar to our MAC protocol, the protocols in [16] [17] employ omni directional RTS and CTS but only one channel is used. Furthermore, the modified MAC protocols in [16] [17] suffer from two main drawbacks: (i) using one channel to transmit/receive omni directional RTS/CTS might interfere with the ongoing data frame transmission. (ii) If omni directional RTS/CTS frames are not allowed to be sent over the range of the ongoing data frame transmission (to prevent collision), the average system throughput will be low.

To overcome the problems and limitations discussed above, Pan *et. al.* [10] proposed a two-channel MAC protocol that takes advantage of the large promised throughput offered by directional antennas. The proposed MAC protocol takes into consideration the hidden terminal problem in mobile ad hoc networks. As opposed to [11]-[14], the proposed directional MAC protocol incorporates the positions of the destination stations as well as the interfering ones in the beamforming process at each mobile station.

### **1.3 Outline of the Thesis**

The rest of the thesis is organized as follows. In chapter two, we briefly review the basic concepts of IEEE 802.11 wireless local area networks and adaptive antenna arrays. We also review the DOA estimation algorithm used in this work.

In chapter three, we evaluate the performance of a typical DMAC protocol when inaccurate DOA information is employed. Our DOA estimation results using the ESPRIT are also presented. In chapter four, we present detailed description for our proposed 2-channel 2-mode DMAC protocol. In chapter five, the simulation results for the proposed protocol are presented and compared to the IEEE 802.11 protocol. Finally, chapter six provides a summary and some directions for future work.

# Chapter 2

## Background

### **2.1 Introduction**

In this chapter, we review some basic concepts related to the IEEE 802.11 standard and adaptive antennas. The background and architecture of the IEEE 802.11 standard are outlined in section 2.2. In section 2.3, some definitions related to antenna arrays are introduced. Finally, the DOAs estimation algorithm is discussed in section 2.4.

### **2.2 IEEE 802.11**

#### **2.2.1 The IEEE 802.11 standard**

The IEEE adopted the first wireless LAN (WLAN) standard, namely the IEEE 802.11 standard [19], in 1997. IEEE 802.11 is a standard for wireless connectivity for fixed, portable, and moving stations within a local area [5]. This standard defines the details of the MAC and physical (PHY) layers for a WLAN. It addresses local area networking where devices communicate with each other within reachable distance over the air.

## 2.2.2 Architecture of the IEEE 802.11 standard

IEEE 802.11 applies at the lowest two layers of the Open System Interconnection (OSI) protocol stack, namely the physical layer and the data link layer. The physical layer standard specifies the signaling techniques used and the implementation of media specific functions. The data link layer defines the frame transmission structure for control, data and management messages and the architecture for data transmission across a WLAN.

As shown in Figure 2.1, mapped to the OSI reference model, the IEEE 802.11 defines two sub-layers of the data link layer: logical link control (LLC) and media access control (MAC). The physical layer consists of three different types: frequency hopping spread spectrum (FHSS), direct sequence spread spectrum (DSSS), and infrared (IR).

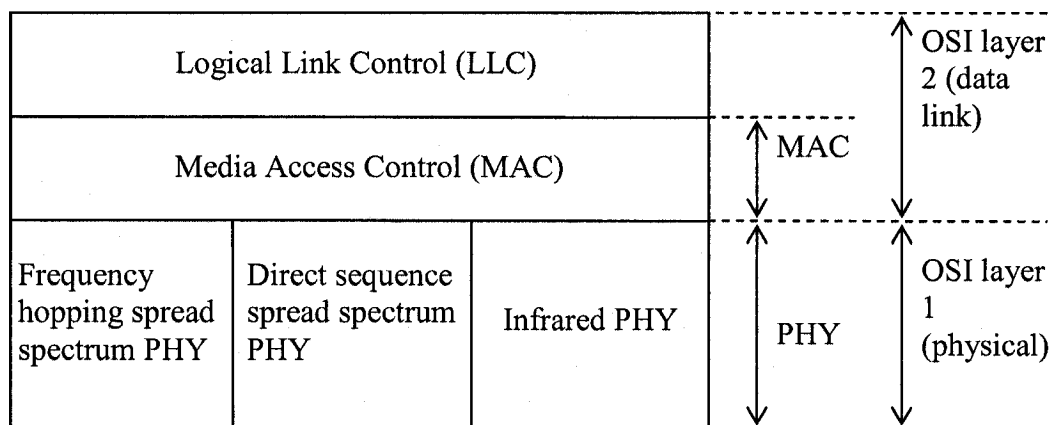


**Figure 2.1 IEEE 802.11 standards mapped to the OSI reference model.**

Typically, the IEEE 802.11 architecture is comprised of several components and services that are defined as follows:

### (i) Wireless LAN Station

The station (STA) is the most basic component of the wireless network. A station is any device that comprises the functionality of the 802.11 protocol which contains MAC

and physical layer to the wireless media. Typically the 802.11 protocols are implemented in a network interface card (NIC).

Normally, a station could be a notebook, computer, an Access Point (AP) or any intelligent wireless terminal that supports all the 802.11 station services such as authentication, privacy, and data transmission.

**(ii) Basic Service Set (BSS)**

IEEE 802.11 defines the Basic Service Set (BSS) as the basic cell of an 802.11 wireless LAN. Similar to a “cell” in pre IEEE terminology, the BSS consists of a group of any number of stations controlled by a single “Coordination Function” (the logical function that determines when a station can transmit or receive). In a BSS, all stations can communicate with each other.

**(iii) Independent Basic Service Set (IBSS)**

The most basic wireless LAN topology is a set of stations, which forms a self-contained network in which no access to a distribution system is available. This form of network topology is referred to as an Independent Basic Service Set (IBSS) or an ad hoc network.

Unlike BSS, in an IBSS, mobile stations communicate directly with each other without an AP, as shown in Figure 2.2. Every mobile station may not be able to communicate with every other station due to the range limitation. There are no relay functions in an IBSS. Therefore all stations need to be within the range of each other. One of the stations in the IBSS can be configured to initiate the network and assume the Coordination Function.

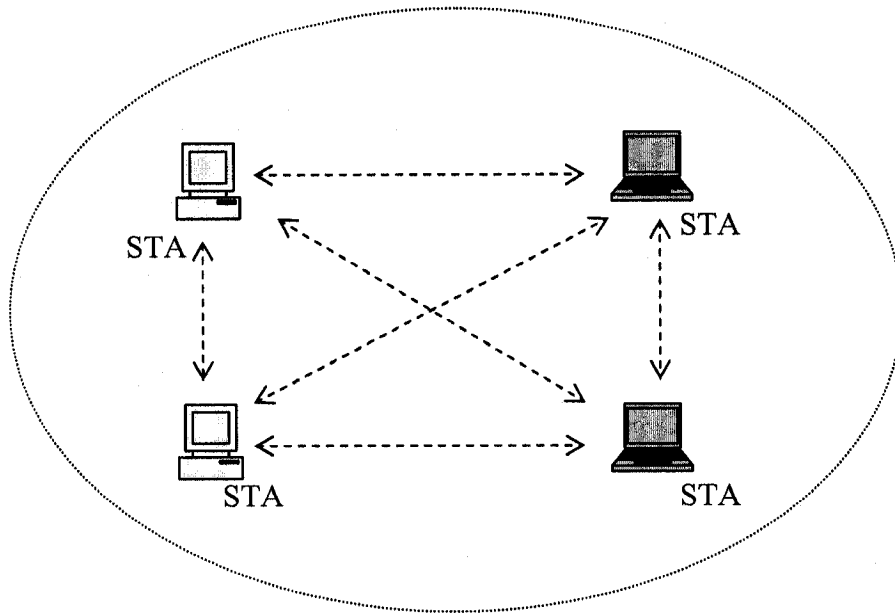


**Figure 2.2 Independent Basic Service Set.**

**(iv) Infrastructure Basic Service Set**

As shown in Figure 2.3, an Infrastructure Basic Service Set is a BSS with an AP. The AP provides a local relay function for the BSS. All stations in the BSS communicate with the AP and no longer communicate directly. This local relay function effectively doubles the range of the IBSS. The AP may also provide connection to a distribution system.

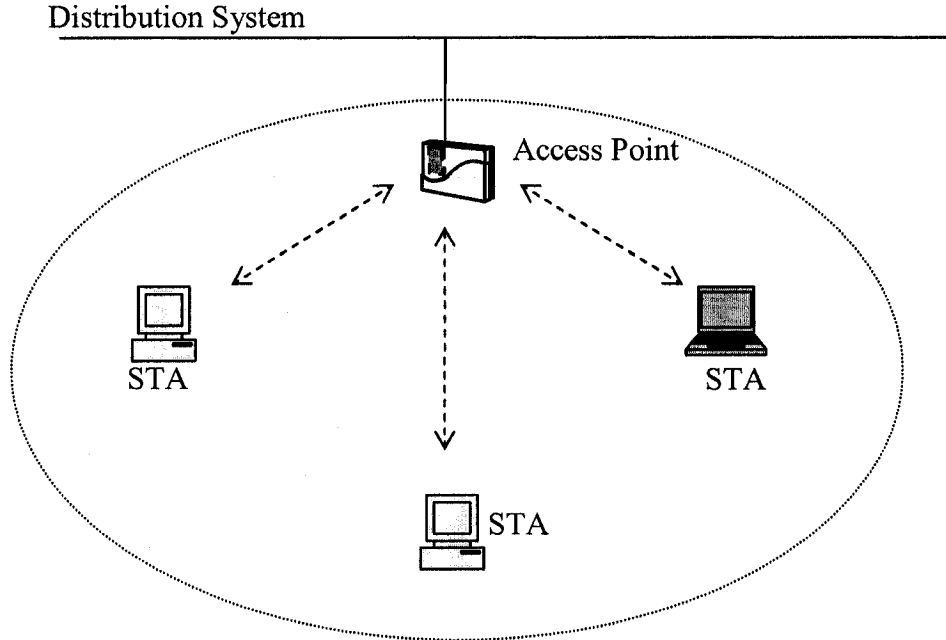


**Figure 2.3 Infrastructure Basic Service Set.**

**(v) Distribution System (DS)**

The distribution system (DS) is a system to interconnect a set of BSSs. Thus, a DS means an AP communicates with another AP to exchange frames for stations in their respective BSSs. As described by IEEE 802.11, the distribution system is implementation independent. DS is not necessarily a network or any restricted type of network. Therefore, the distribution system may be a wired network like IEEE 802.3 Ethernet networks, IEEE 802.4 token bus networks, or a special purpose box that interconnects the APs and provides the required distribution services.

**(vi) Extended Service Set (ESS)**

Using the Extended Service Set, IEEE 802.11 extends the range of mobility to an arbitrary range. An ESS is a set of infrastructure BSS's interconnected by a DS, where

the APs communicate amongst themselves to forward traffic from one BSS to another (see Figure 2.4).

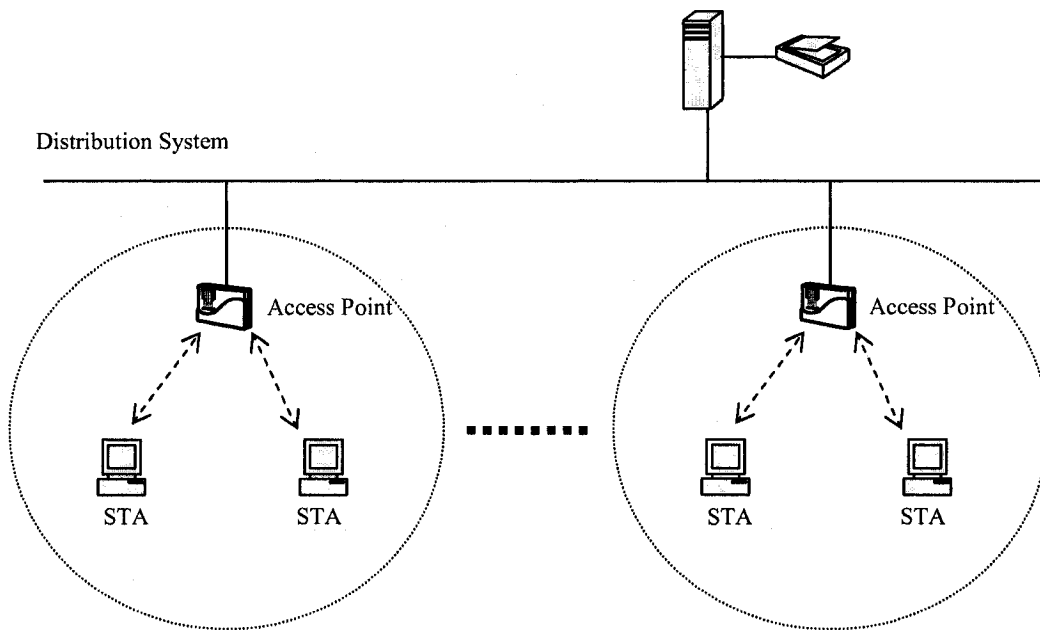


**Figure 2.4 Extended Service Set.**

DS is the backbone of the wireless LAN and may be constructed using either a wired LAN or wireless network. Typically, the DS determines the destination for traffic received from a BSS. The DS also determines if traffic should be relayed back to a destination in the same BSS, or forwarded on the DS to another AP, or sent into the wired network to a destination not in the ESS. Communications received by an AP from the DS are transmitted to the BSS to be received by the destination mobile station.

Other network users outside of the ESS consider the ESS and all of its mobile stations as a single MAC layer network where all stations are physically stationary. Thus, the ESS hides the mobility of the mobile stations from other users outside the ESS and it also allows other users that might not support the IEEE 802.11 protocol to communicate with

wireless terminals in a wireless LAN. In another words, the ESS can hide the mobility of wireless stations from other networks.

### 2.2.3 Frames Structure of the IEEE 802.11

There are three main types of frames in IEEE 802.11: data frames, control frames, and management frames. Data frames are used for data transmission. Control frames are used for handshaking and for positive acknowledgements during the data exchange (e.g. RTS, CTS, and ACK), and management frames are used for station association and disassociation with the AP, timing, synchronization, authentication and deauthentication.

According to their specific function, each frame type is subdivided into different subtypes. Figure 2.5 shows the general MAC frame format.

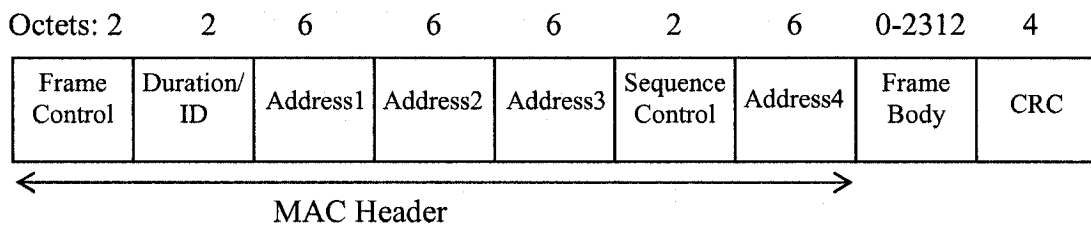


**Figure 2.5 MAC Farme Format.**

As shown in Figure 2.6, The Frame Control field in the MAC header is 16 bits long. The Duration/ID field in the MAC header is 16 bits long and is used in two ways. It usually contains a duration value (net allocation vector) that is used in the MAC protocol.

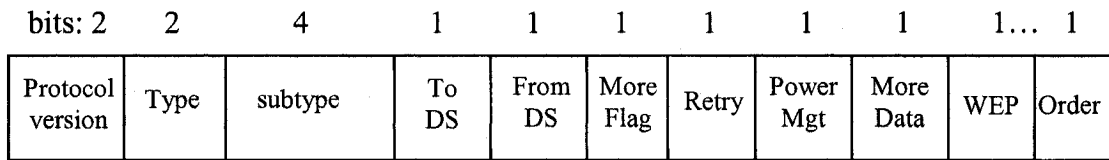


**Figure 2.6 Frame Control Field.**

The use of the 4 Address fields is specified by the To DS and From DS fields in the Frame Control field (see Figure 2.6). Addresses are 48-bit-long IEEE 802.11 MAC addresses, and can be individual or group (multicast/broadcast). The Address 1 field in this case contains the destination address. The BSS identifier (BSS ID) is a 48-bit field, of the same format as IEEE 802.11 MAC addresses, uniquely identifies a BSS, and is given by the MAC address of the station in the AP of the BSS. The destination address is an IEEE MAC individual or group address that specifies the MAC entity of the final recipient of the MSDU that is contained in the Frame Body field. The source address is a MAC individual address that identifies the MAC entity from intended immediate recipient station for the MAC PDU (MPDU) in the Frame Body field. The transmitter address is a MAC individual address that identifies the station that transmitted the MPDU contained in the frame body field.

The Sequence Control field is 16 bits long, and it provides 4 bits to indicate the number of each fragment of an MSDU and 12 bits of sequence numbering for a sequence number space of 4095. The Frame Body field contains information of the type and subtype specified in the Frame Control field. For Data type frames, the Frame Body field contains an MSDU or a fragment of a MSDU. Finally, the CRC field contains the 32-bit cyclic redundancy check calculated over the MAC header and Frame Body field.

## 2.2.4 MAC layer of IEEE 802.11

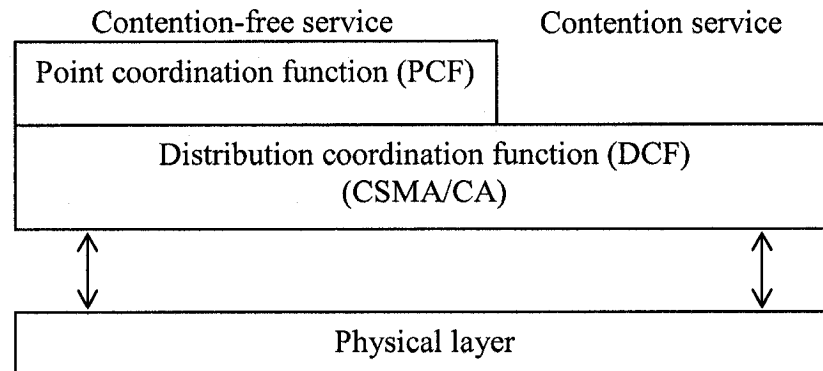


**Figure 2.7 IEEE 802.11 MAC architecture.**

The MAC layer defines two different access methods, the Distributed Coordination Function (DCF) and the Point Coordination Function (PCF). DCF provides support for asynchronous data transfer of MSDUs on a best-effort basis. Under this function, the transmission medium operated in the contention mode, requiring all stations to contend for the channel for each transmitted packet. The IEEE 802.11 also defines an optional PCF which may be implemented by an AP, to support connection-oriented time-bounded transfer of MSDUs. The medium can alternate between the contention period (CP), during which the medium used contention mode, and a contention-free period (CFP). During the CFP, the medium usage is controlled by the AP, thereby eliminating the need for stations to contend for the channel access.

### 2.2.4.1 Distributed Coordination Function (DCF)

The DCF is the basic access method used to support asynchronous data transfer on a best-effort basis. All stations are required to support the DCF. The access control in ad

hoc networks uses only the DCF. Infrastructure networks can operate using just the DCF or a coexistence of the DCF and PCF.

The DCF is based on the CSMA/CA protocol. Carrier sensing involves monitoring the channel to determine whether the medium is idle or busy. If the medium is busy, the station should wait until the channel becomes idle. When this happens, there is a problem: other stations may have also been waiting for the channel to become idle. If the protocol is to transmit immediately after the channel becomes idle, then collisions are likely to occur; and because collision detection is not possible, the channel will be wasted for the collision. A solution to this problem is to randomize the times at which the contending stations attempt to occupy the channel. Figure 2.8 shows the basic CSMA/CA operation.

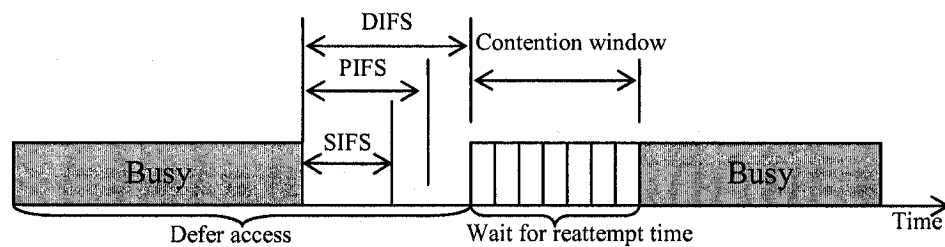


**Figure 2.8 Basic CSMA/CA operations.**

All stations are obliged to remain quiet for a certain minimum period after a transmission has been completed, called the inter frame space (IFS). High priority frames must only wait for the short IFS (SIFS) period before they contend again for the channel. The PCF IFS (PIFS) is intermediate in duration and is used by the PCF to gain priority access to the channel at the start of a CFP. The DCF IFS (DIFS) is used by the DCF to transmit data and management MDPUs.

A CSMA protocol works as follows:

1. A station desiring to transmit must sense the channel. If the channel is busy, i.e., the channel is used by some other stations, then the station defers its transmission to a later time. If the channel is sensed idle for a period of DIFS then the station can use channel to transmit.

2. The receiving station checks the CRC of the received packet and sends an acknowledgment (ACK). Receipt of the acknowledgment means there was no collision occurred during this period. If sender does not receive the ACK then it retransmits the packet until it receives ACK or the packet is thrown away after a given number of retransmissions.

In order to reduce the probability of two stations colliding because they cannot hear each other, the standard employs a Virtual Carrier Sense (VCS) mechanism. A station, wanting to transmit a packet, firstly transmits a short control packet called Request To Send (RTS), which includes the source, destination, and the duration of the following transaction. The destination station responds if the medium is free with a response control packet called Clear to Send (CTS), which includes the same information. All stations receiving either the RTS and/or the CTS, set their Virtual Carrier Sense indicator (called NAV, for Network Allocation Vector), according to the given duration provided by the frames. This information is used to schedule the time for their next channel sense action. This process reduces the probability of collision at the receiver area. This is simply because a station that did not receive the RTS transmission can hear the CTS and mark the channel as busy until the end of the transmission. The duration information on the RTS also protects the transmitter area from collisions during the ACK (from stations that

are out of range of the ACK frame). The following diagram show a transmission process between stations, and the NAV setting of their neighbors.

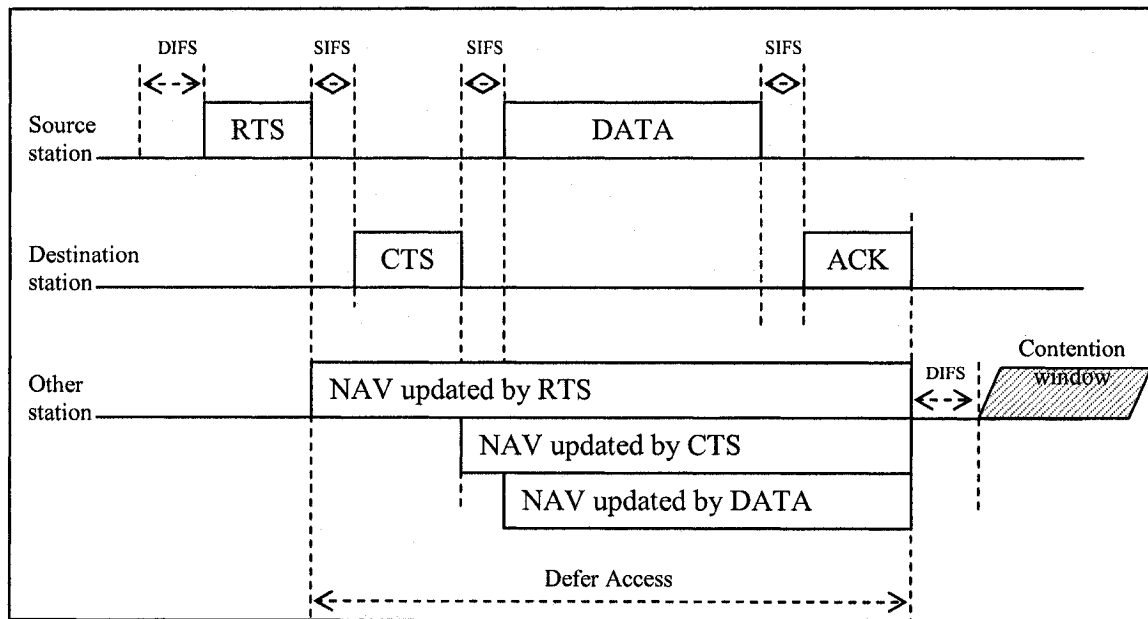


**Figure 2.9 Timing diagram for a transmission process.**

Due to the fact that the RTS and CTS are shorter than DATA frames, the mechanism can avoid the unnecessary bandwidth waste due to long collision time. These short frames are recognized faster than if the whole packet was to be transmitted. This is significant if the packet is much larger than the RTS, The 802.11 standard also allows for short packets to be transmitted without the RTS/CTS. This is controlled by a parameter called RTS Threshold in every station.

#### **2.2.4.2 Point Coordination Function (PCF)**

The PCF function is performed by the point coordinator (PC) in the AP within a BSS. The PCF is required to coexist with the DCF and it logically sits on top of the DCF as shown in Figure 2.7. The CPF repetition interval determines the frequency to contention-free traffic, and the remainder is provided for contention-based traffic. The CFP

repetition is initiated by a beacon frame, where the beacon frame is transmitted by the AP. Figure 2.10 shows the structure of the CFP repetition interval, illustrating the coexistence of the PCF and DCF.

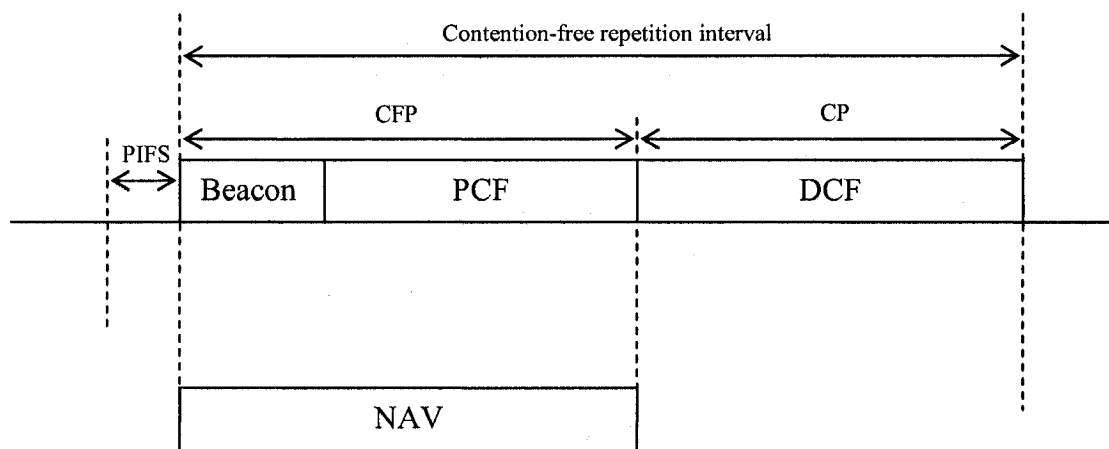


**Figure 2.10 Point coordination frame transfer.**

It is up to the AP to determine how to operate the CFP during any given repetition interval. If traffic is very light, the AP may shorten the CFP and provide the remainder of the repetition interval for the DCF. The CFP may also be shortened if DCF traffic from the previous repetition interval carries over into the current interval.

### 2.2.5 Physical Layer

The IEEE 802.11 LAN has three techniques defined to operate with its MAC layer: frequency hopping spread spectrum (FHSS), direct sequence spread spectrum (DSSS), and infrared (IR). In what follow, we give an overview of these three techniques.

### **2.2.5.1 Frequency hopping spread spectrum**

Spread spectrum (SS) provides a great robustness with respect to interference as well as other transmission impairments such as fading that results from multipath propagation. Frequency hopping (FH) is one type of spread spectrum techniques. FHSS uses 79 non-overlapping 1 MHz channels to transmit a 1 Mbps data signal over the 2.4 GHz Industrial/Scientific/Medical (ISM) band. Another option is provided for transmission at a rate of 2 Mbps. This band occupies the range from 2400 to 2483.5 MHz, providing 83.5 MHz bandwidth. The standard defines 78 hopping patterns that are divided into 3 sets of 26 patterns each. Each hopping pattern jumps a minimum of 6 channels in each hop. Each 802.11 network must use a particular hopping pattern. The hopping patterns allow up to 26 networks to coexist and operate simultaneously.

### **2.2.5.2 Direct sequence spread spectrum**

Direct sequence spread spectrum (DSSS) is a method for taking a data signal of a given bit rate and modulating it into a signal that occupies a much larger bandwidth. The DSSS transmission system takes 1 Mbps data signal and converts it into 11 Mbps signal using Binary Phase Shift Keying (BPSK) modulation. Eleven channels have been defined to operate in the 2.4 GHz ISM band. Channels can operate without interfering with each other by at least 30MHz gap. DSSS defines an option for 2 Mbps operation using QPSK modulation.

### **2.2.5.3 Infrared**

The IEEE 802.11 infrared physical layer operates in the near-visible light range of 850 to 950 nanometers. Diffuse transmission is used so that the transmitter and receivers

do not have to point to each other. The transmission distance is limited to the range of 10 to 20 meters, and the system cannot operate outdoors. The transmission system uses pulse-position modulation (PPM) in which the binary data is mapped into symbols that consist of a group of slots. The 1 Mbps data system uses a 16 PPM slot. The 2 Mbps data system uses a 4 PPM in which groups of two data bits are mapped into four-slot symbol.

## **2.3 Adaptive Antennas**

The adaptive antenna technology is based on antenna arrays where the radiation pattern is altered by adjusting the amplitude and relative phase on the different array elements. Electrically steerable antenna beampatterns are most often generated by using array antennas. Generally, any combination of elements can form an array. However, usually equal elements in a regular geometry are used.

### **2.3.1 Uniformly Spaced Linear Antenna Array**

Using an antenna array, it is possible to obtain a very good control of the radiation pattern. One of the simplest geometries is the one-dimensional linear equidistant array where all the array elements are placed along a line with equal distance between them as shown in Figure 2.11.

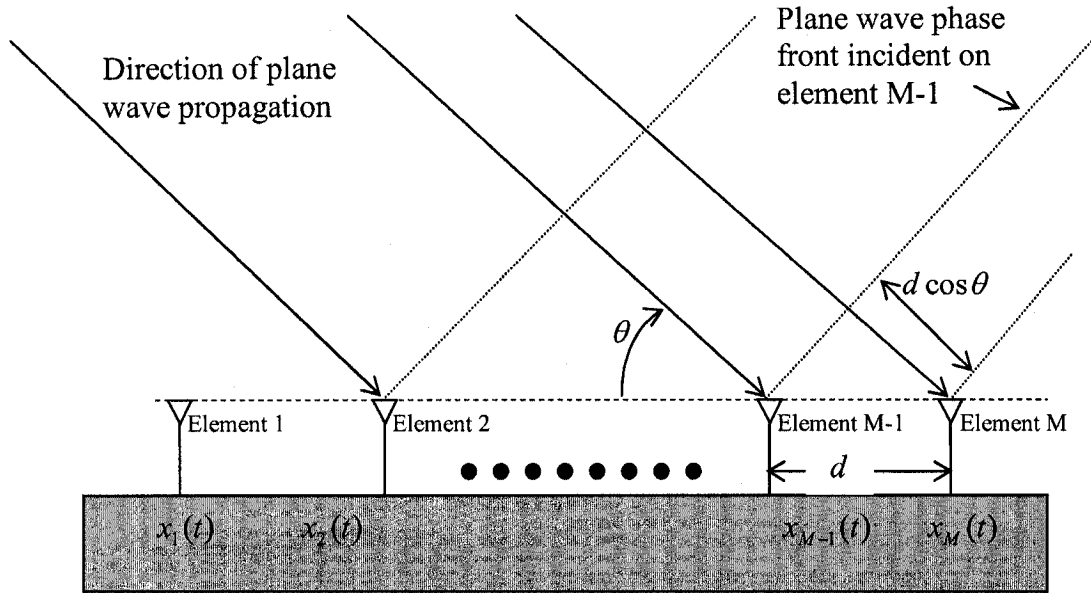


**Figure 2.11 An M-element uniformly spaced linear array**

In the discussion that follows, the signal is assumed to be narrowband. As shown, the elements are separated by a distance  $d$ . Consider a plane wave incident on the array with an angle  $\theta$  relative to the axis of the array.  $\theta$  is called the direction of arrival (DOA) of the incoming signal. The received signal at the first element can be expressed as

$$z_1(t) = \alpha(t) \cos(2\pi f_c t + \phi(t) + \delta) \quad (2.1)$$

where  $\alpha(t)$  is the amplitude of the signal,  $f_c$  is the signal carrier frequency,  $\phi(t)$  is the phase of information component and  $\delta$  is a random phase. Equation (2.1) can be represented by complex envelope as follows

$$x_1(t) = \alpha(t) \exp(j(\phi(t) + \delta)). \quad (2.2)$$

As shown in Figure 2.1, we take the first element as a reference point. We notice that the plane wave arriving at the second element will travel  $d \cos \theta$  distance more than that arrived at the first element. The time delay associated with this distance is given by

$$\tau = \frac{d \cos \theta}{C} \quad (2.3)$$

where  $C$  is the speed of light. Thus the signal received at the second element can be expressed as

$$z_2(t) = z_1(t - \tau) = \alpha(t - \tau) \cos(2\pi f_c(t - \tau) + \phi(t - \tau) + \delta). \quad (2.4)$$

Since the carrier frequency is larger than the channel bandwidth, then we have

$$z_2(t) = \alpha(t) \cos(2\pi f_c t - 2\pi f_c \tau + \phi(t) + \delta) \quad (2.5)$$

and the complex envelope of  $z_2(t)$  is given by

$$\begin{aligned} x_2(t) &= \alpha(t) \exp(j(-2\pi f_c \tau + \phi(t) + \delta)) \\ &= x_1(t) \exp(-j2\pi f_c \tau). \end{aligned} \quad (2.6)$$

We can see that the distance difference at different elements leads to the phase shift in the received signal. From equations (2.3) and (2.6), we have

$$\begin{aligned} x_2(t) &= x_1(t) \exp(-j2\pi f_c \frac{d \cos \theta}{V_c}) \\ &= x_1(t) \exp(-j \frac{2\pi}{\lambda} d \cos \theta) \end{aligned} \quad (2.7)$$

where  $\lambda$  is the wavelength of the carrier wave. The received signal at the  $i^{\text{th}}$  element can then be presented as

$$x_i(t) = x_1(t) \exp(-j \frac{2\pi}{\lambda} (i-1) d \cos \theta), \quad i = 1, 2, \dots, M. \quad (2.8)$$

Let

$$x(t) = \begin{bmatrix} x_1(t) \\ x_2(t) \\ \vdots \\ x_M(t) \end{bmatrix} \quad (2.9)$$

and

$$a(\theta) = \begin{bmatrix} 1 \\ \exp(-j \frac{2\pi}{\lambda} d \cos \theta) \\ \vdots \\ \exp(-j \frac{2\pi}{\lambda} (M-1) d \cos \theta) \end{bmatrix}. \quad (2.10)$$

From (2.9) and (2.10), equation (2.8) can be expressed as

$$x(t) = a(\theta)x_1(t) \quad (2.11)$$

where  $x(t)$  is called the array input vector and  $a(\theta)$  is called the steering vector.

In general, more than one signal can arrive at the antenna array at the same time. We assume that there are  $K$  narrowband signals  $s_1(t), \dots, s_K(t)$  impinging on the array with DOA  $\theta_i, i = 1, 2, \dots, K$ . At the receiver, the received signal can be expressed as

$$x(t) = \sum_{i=1}^K a(\theta_i)s_i(t) + n(t) \quad (2.12)$$

where

$$a(\theta_i) = \begin{bmatrix} 1 \\ \exp(-j \frac{2\pi}{\lambda} d \cos \theta_i) \\ \vdots \\ \exp(-j \frac{2\pi}{\lambda} (M-1) d \cos \theta_i) \end{bmatrix} \quad (2.13)$$

and  $n(t)$  is  $K \times 1$  noise vector at the array element. The received signal can be express in vector form as

$$x(t) = a(\theta)s(t) + n(t) \quad (2.14)$$

where

$$a(\theta) = [a(\theta_1), \dots, a(\theta_k)]$$

and

$$s(t) = \begin{bmatrix} s_1(t) \\ \vdots \\ s_k(t) \end{bmatrix}. \quad (2.15)$$

### 2.3.2 Beamforming of Adaptive Antenna

Adaptive beamforming is a technique in which the antenna array is able to achieve maximum reception in a specified direction by estimating the signal arrival from a desired direction and rejecting other signals of the same frequency from other directions. This can be achieved by varying the complex weight of each element used in the antenna array. Although signals coming from different transmitters occupy the same frequency channel, they still arrive from different directions. The function of the complex weights  $W$  of the antenna elements is to shift the peaks of the antenna beam pattern to the direction of desired signal and the nulls to the other signals (interfering signals). In a simple case, the weights may be chosen to give one central beam in some direction, e.g., in the direction of a desired node. The weights can then be slowly changed to steer the beam until maximum signal strength occurs, and the direction of the signal source is found.

To illustrate different beamforming aspects, we consider the adaptive beamforming configuration shown in Figure 2.12.

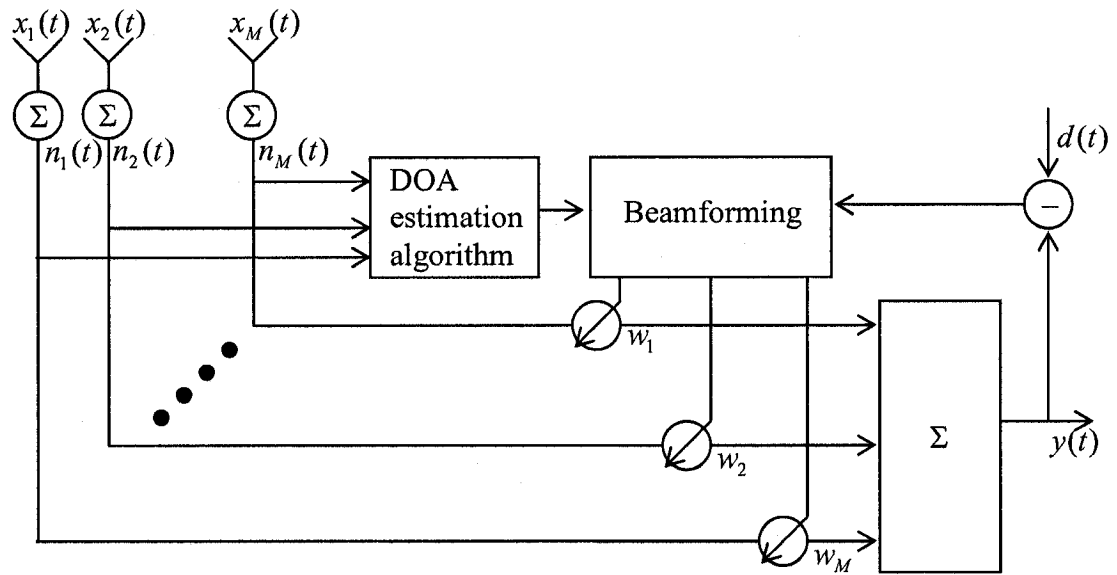


**Figure 2.12 A simple narrowband adaptive array system.**

The output of the antenna array,  $y(t)$ , is the weighted sum of the received signals  $x_i(t)$  at the array elements and the noise  $n_i(t)$  at the receivers connected to each element. The weights  $w_i$ ,  $i = 1, 2, \dots, M$  are iteratively computed based on the array output  $y(t)$ , a reference signal  $d(t)$  that approximates the desired signal, and previous weights. The reference signal is approximated to the desired signal using a training sequence or a spreading code, which is known at the receiver. The format of the reference signal depends on the system where adaptive beamforming is being used. The reference signal usually has a good correlation with the desired signal and the degree of correlation influences the accuracy and the convergence of the algorithm.

The array output is given by

$$y(t) = \sum_{i=1}^M w_i x_i(t). \quad (2.16)$$

Equation (2.16) can also be expressed in vector form as

$$y(t) = w^H x(t) \quad (2.17)$$

where

$$w = \begin{bmatrix} w_1 \\ w_2 \\ \vdots \\ w_M \end{bmatrix}$$

and  $H$  denotes the complex conjugate transpose of the weight vector  $w$ .

In order to compute the optimum weights, the array response vector from the sampled data of the array output has to be known. The array response vector is a function of the incident angle as well as the frequency. The baseband received signal at the  $i^{\text{th}}$  antenna is a sum of phase-shifted and attenuated versions of the original signal  $x_1(t)$ . This has been illustrated by equation (2.8).

To have a better understanding, re-write  $x(t)$  in equation (2.14) by separating the desired signal from the interfering signals. Let  $s(t)$  denote the desired signal arriving at an angle of incidence  $\theta_0$  at the array and the  $u_i(t)$  denotes the  $K_u$  number of undesired interfering signals arriving at angles of incidence  $\theta_i$ ,  $i = 1, \dots, K_u$ . It must be noted that, in this case, the directions of arrival are known a priori using a direction of arrival (DOA) algorithm.

The output of the antenna array  $x(t)$  can now be re-written as

$$x(t) = a(\theta_0)s(t) + \sum_{i=1}^{K_u} a(\theta_i)u_i(t) + n(t) \quad (2.18)$$

where  $a(\theta_i)$  is the array propagation vector of the  $i^{\text{th}}$  interfering signal, and  $a(\theta_0)$  is the array propagation vector of the desired signal. Therefore, having the above information,

adaptive algorithms are required to estimate  $s(t)$  from  $x(t)$  while minimizing the error between the estimate  $\hat{s}(t)$  and the original signal  $s(t)$ .

Let  $d(t)$  represent a signal that is closely correlated to the original desired signal  $s(t)$ .  $d(t)$  is referred to as the reference signal. The mean square error (MSE) between the beamformer output and the reference signal can now be computed as

$$E\{e^2(t)\} = E\{[d^*(t) - w(t)^H x(t)]^2\}, \quad (2.19)$$

where  $*$  is the conjugate operator. Thus we have

$$E\{e^2(t)\} = E\{[d^2(t) - 2w(t)^H r + w(t)^H R w(t)]\} \quad (2.20)$$

where  $r = E\{[d^*(t)x(t)]\}$  is the cross-correlation vector between the desired signal and the received signal, and  $R = E[x(t)x^H(t)]$  is the auto-correlation matrix of the received signal also known as the covariance matrix. The minimum MSE can be obtained by setting the gradient vector of the above equation, with respect to  $w$ , to zero, i.e.

$$\nabla_w (E\{e^2(t)\}) = -2r + 2Rw. \quad (2.21)$$

Therefore the optimum solution for the weight  $w_{opt}$  is given by

$$w_{opt} = R^{-1}r \quad (2.22)$$

This equation is referred to as the optimum Weiner solution [42].

Assume that node A wants to send data to node B in directional mode with DOA equal to 125 degrees as shown in Figure 2.13. Figure 2.14 shows a typical antenna beam pattern for number of element (NOE) =5 antenna array that can be used by node A for data transmission after antenna beamforming. The main lobe of the beam pattern has been shifted to the desired direction.

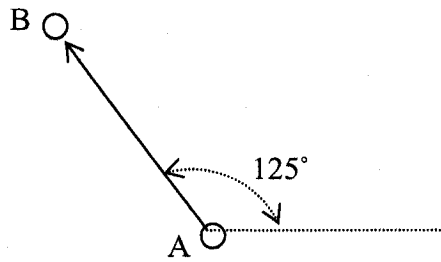


**Figure 2.13** An example where desired DOA=125 deg.

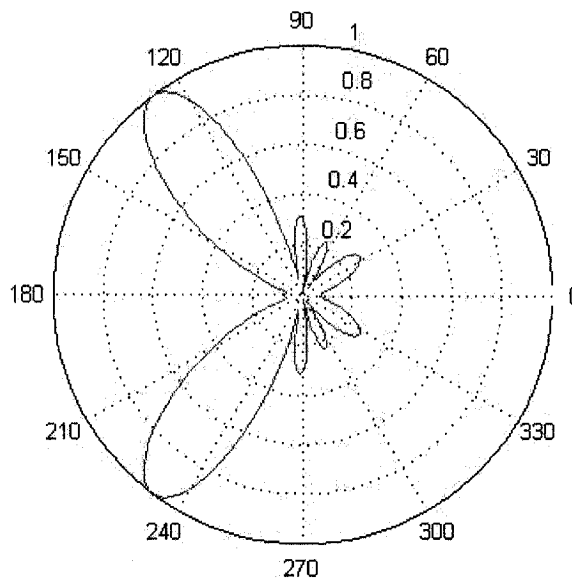


**Figure 2.14** Transmitter's beampattern, NOE=5,  $\lambda/2$  spacing between antennas, desired DOA=125 deg.

Another advantage of adaptive antennas is the ability to form nulls at interference directions while transmitting at the desired direction. In fact, given  $M$  elements, an antenna can form up to  $M - 1$  nulls [41].

In the scenario shown in Figure 2.15, node C belongs to one of another ongoing transmission pair. Assuming that the DOA from A to C is 30 degrees, node A can eliminate unwanted direction in the antenna beampattern for 5-element array shown as Figure 2.16.

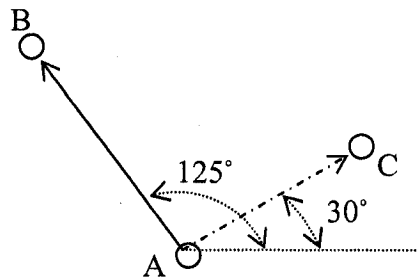


**Figure 2.15** An example, desired DOA=125 deg, undesired DOA=30 deg.

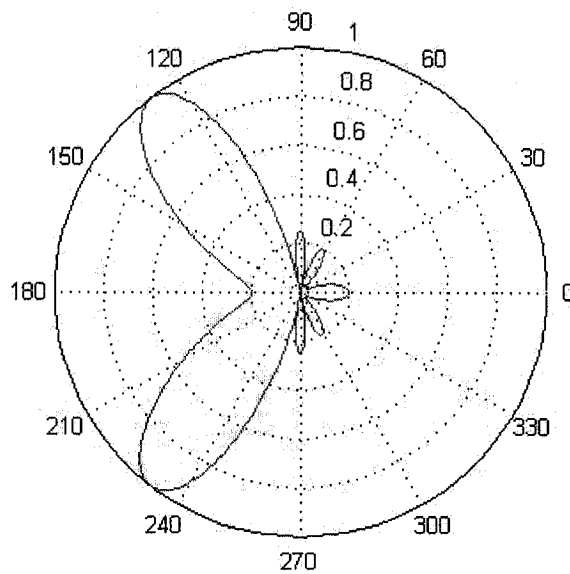


**Figure 2.16** Transmitter's beampattern, NOE=5,  $\lambda/2$  spacing between antennas, desired DOA=125 deg, undesired DOA = 30 deg.

As shown in Figure 2.16, the main lobe is still focused towards the desired destination. At the same time, unlike Figure 2.14, the antenna beam pattern has a null in the 30 degrees direction. Thus any signal from this direction will not affect the signal transmitted from node A. Also, the signal from node A will not affect other ongoing transmissions by node C.

### **2.3.3 Adaptive Algorithm**

Based on information or reference signal required, adaptive algorithms can be classified into 2 categories [26].

1. Non-blind adaptive algorithms: This class of algorithms is based on minimization of the mean square error between the received signal and the reference signal. Therefore it is required that a reference signal, with high correlation with the desired signal, to be available. Examples of algorithms in this class include the least mean square (LMS) algorithm [27] and the recursive least square (RLS) algorithm [30]. Reference signals required for the above algorithms are generated in several ways. In TDMA, every frame consists of a sequence, which can be used as a reference signal. In digital communication, synchronization signals can be used for the same purpose.

2. Blind adaptive algorithms: These algorithms do not require any reference signal information. They themselves generate the required reference signal from the received signal to get the desired signal. Examples of algorithms in this class include the constant modulus algorithm (CMA) [32], the Code Filtering Approach (CFA) [33] algorithm.

### 2.3.3.1 Least Mean Squares

The Least Mean Square (LMS) algorithm, introduced by Widrow and Hoff in 1959 [27], is an adaptive algorithm, which uses a gradient-based method of steepest decent [28]. LMS algorithm uses the estimates of the gradient vector from the available data. It incorporates an iterative procedure that makes successive corrections to the weight vector in the direction of the negative of the gradient vector which eventually leads to the minimum mean square error. A significant feature of the LMS algorithm is its simplicity; it does not require measurements of the pertinent correlation function, nor does it require matrix inversions.

From the method of steepest descent, the weight vector is given by [29],

$$w(n+1) = w(n) + \frac{1}{2} \mu [-\nabla(E\{e^2(n)\})] \quad (2.23)$$

where  $\mu$  is the step-size parameter which controls the convergence characteristics of the LMS algorithm. Combining equations (2.18) and (2.23), the weight update is given by,

$$w(n+1) = w(n) + \mu x(n)[d^*(n) - x^h(n)w(n)] = w(n) + \mu x(n)e^*(n). \quad (2.24)$$

The LMS algorithm is initiated with an arbitrary value  $w(0)$  for the weight vector at  $n=0$ . The successive corrections of the weight vector eventually lead to the minimum value of the mean squared error. The LMS algorithm can be summarized as followings

$$y(n) = w^h x(n) \quad (2.25)$$

$$e(n) = d^*(n) - y(n) \quad (2.26)$$

$$w(n+1) = w(n) + \mu x(n)e^*(n) \quad (2.27)$$

if  $\mu$  is chosen to be very small then the algorithm converges very slowly. A large value of  $\mu$  may lead to a faster convergence but may be less stable around the minimum value.

### **2.3.3.2 Recursive least squares (RLS) algorithm**

Different from the LMS algorithm, which uses the method of steepest descent to update the weight vector, the RLS algorithm [30] uses the method of least squares to adjust the weight vector.

An important feature of the RLS algorithm is that it utilizes information contained in the input data, extending back to the instant of time when the algorithm is initiated. The RLS algorithm converges with an order of magnitude faster than the LMS algorithm if the Signal to Noise Ratio (SNR) is high.

### **2.3.3.3 Constant modulus algorithm (CMA)**

The constant modulus algorithm is a blind adaptive algorithm proposed by Goddard [32] and by Treichler and Agee [36] [38]. It requires no previous knowledge of the desired signal. Instead, it exploits the constant or nearly constant amplitude properties of most modulation formats used in wireless communication. By forcing the received signal to have constant amplitude, CMA recovers the desired signal.

## **2.4 *Direction of Arrival (DOA) estimation algorithms***

The goal of DOA estimation is to use the data received at the array to estimate the signal direction of arrival. The results of DOA estimation are then used by the array to design the adaptive beamformer which is used to maximize the power radiated towards the intended receiver, and to introduce nulls to combat interference as was explained in the previous section.

Various techniques of DOA estimation for electromagnetic waves have been developed in the literature [20]-[24]. Examples of these techniques include the Multiple Signal Classification (MUSIC) [20], Root-MUSIC [21], Unitary Spectral MUSIC, Unitary Root-MUSIC, Estimation of Signal Parameter via Rotational Invariance Technique (ESPRIT) [22], TLS ESPRIT [23] and Unitary ESPRIT [24].

Among the above algorithms, the ESPRIT algorithm is one of the widely used algorithms for DOA estimation where it offers many advantages. Few to mention are,

1. ESPRIT is more effective from computational point of view.
2. Unlike different MUSIC algorithms, ESPRIT does not suffer from the many false peaks in the spatial spectrum [23].

#### **2.4.1 Data Model of ESPRIT**

The idea behind ESPRIT is to divide the antenna array into two equivalent sub-arrays separated by a known displacement. It uses two identical arrays in the sense that array elements need to form matched pairs with an identical displacement vector. That is, the second element of each pair ought to be displaced by the same distance and in the same direction relative to the first element.

Although ESPRIT needs two equivalent sub-arrays, this does not mean that one has to have two separate arrays. The array geometry should be such that the elements could be selected to have this property. For example, if the antenna above has five identical elements with an inter-element spacing, it may be thought of as two arrays of four matched pairs, one with the [1 2 3 4] elements and one with the [2 3 4 5] elements. The two arrays are displaced by the distance  $d$ . The way that ESPRIT exploits this sub array structure for DOA estimation is now briefly described.

Consider a uniform linear array (ULA) as shown in Figure 2.1. The ULA consists of  $M$  equally spaced elements that receive signals transmitted from  $K$  ( $K < M$ ), narrowband sources which are in the far-field of the array. These received signals are assumed to be impinging on the array from directions  $\theta_1, \dots, \theta_K$ .

Denote the signals induced on the  $l^{\text{th}}$  pair (of the two separate arrays) due to a narrowband source in direction  $\theta$  by  $x_l(t)$  and  $y_l(t)$  respectively. The phase difference between these two signals depends on the time taken by the plane wave arriving from the source under consideration to travel from one element to the other. As the two elements are separated by the displacement  $d$ , it follows that

$$y_l(t) = x_l(t) \exp(j2\pi(d/\lambda) \cos \theta) \quad (2.28)$$

Let  $x(t)$  and  $y(t)$  denote the signals received by the two arrays, then we have

$$x(t) = As(t) + n_x(t) \quad (2.29)$$

and

$$y(t) = A\phi s(t) + n_y(t) \quad (2.30)$$

where  $A = [a(\theta_1) \dots a(\theta_K)]$  is the  $(M-1) \times K$  matrix of steering vectors. With its columns denoting the  $K$  steering vectors corresponding to  $K$  directional sources associated with the first sub-array, and  $\phi$  is a  $K \times K$  diagonal matrix, with its  $k^{\text{th}}$  diagonal element given by

$$\phi_{kk} = \exp(j2\pi(d/\lambda) \cos \theta_k). \quad (2.31)$$

In equation (2.30),  $s(t)$  denotes  $K$  source signals induced on a reference element, and  $n_x(t)$ ,  $n_y(t)$  denote the noise induced on the antenna elements of the two sub-arrays, respectively.

Let  $\Gamma_x$  and  $\Gamma_y$  denote two  $(M-1) \times K$  matrices with their columns denoting the  $K$  eigenvectors corresponding to the largest eigenvalues of the two array correlation matrices  $R_{xx}$  and  $R_{yy}$ , respectively. As these are two sets of eigenvectors span the same  $K$  dimensional signal space, it follows that these two matrices  $\Gamma_x$  and  $\Gamma_y$  are related by a unique nonsingular transformation matrix  $\psi$ . That is

$$\Gamma_y = \Gamma_x \psi . \quad (2.32)$$

Similarly, these matrices are related to the  $A$  and  $A\phi$  by another unique nonsingular transformation matrix  $T$ , as the same signal subspace is spanned by these steering vectors.

Thus

$$\Gamma_x = AT \quad (2.33)$$

and

$$\Gamma_y = A\phi T . \quad (2.34)$$

Substituting for  $\Gamma_x$  and  $\Gamma_y$ , and by noting that  $A$  is of full rank, one obtains

$$T\psi T^{-1} = \phi \quad (2.35)$$

which states that the eigenvalues of  $\psi$  are equal to the diagonal elements of  $\phi$  and that the columns of  $T$  are eigenvectors of  $\psi$ . This is the main equation in the development of ESPRIT. It requires an estimate of  $\psi$  from the measurement  $x(t)$  and  $y(t)$ . An eigen

decomposition of  $\psi$  gives its eigenvalues, and equating them to  $\phi$  leads to the DOA estimates

$$\theta_k = \cos^{-1} \left[ \frac{\text{Arg}(\phi_k)}{2\pi(d/\lambda)} \right], k = 1, \dots, K. \quad (2.36)$$

How one obtains an estimate of  $\psi$  from the array signal measurements efficiently has led to many different versions of ESPRIT. One version, referred to as Total Least Squares TLS ESPRIT, is summarized as below [23],

- Make measurements from two identical subarrays, which are displaced by  $d/\lambda$ .
- Estimate the two array correlation matrices from the measurements and find their eigenvalues and eigenvectors.
- Find the number of directional sources  $K$ .
- Form the two matrices with their columns being  $K$  eigenvectors associated with the largest eigenvalues of each correlation matrix. Let these be denoted by  $\Gamma_x$  and  $\Gamma_y$ . For a ULA, this could be done by first forming an  $L$  by  $K$  matrix  $\Gamma$  by selecting its columns as the  $K$  eigenvectors associated with the largest eigenvalues of the estimated array correlation.
- Compute the eigen decomposition of the  $2K \times 2K$  matrix

$$\begin{bmatrix} \Gamma_x^H \\ \Gamma_y^H \end{bmatrix} \begin{bmatrix} \Gamma_x & \Gamma_y \end{bmatrix} = V \Lambda V^H \quad (2.37)$$

Then find its eigenvectors. Let these eigenvectors be the columns of a matrix  $V$ .

- Partition  $V$  into  $K$  by  $K$  sub-matrices as

$$V = \begin{bmatrix} V_{11} & V_{12} \\ V_{21} & V_{22} \end{bmatrix}. \quad (2.38)$$

- Calculate the eigenvalues  $\phi_k$  of the matrix

$$[\phi_k] = -V_{11}V_{22}^{-1}, \quad k = 1, 2, \dots, K. \quad (2.39)$$

- Estimate the direction of arrival

$$\theta_k = \cos^{-1} \left[ \frac{\text{Arg}(\phi_k)}{2\pi(d/\lambda)} \right], \quad k = 1, \dots, K. \quad (2.40)$$

## 2.5 Summary

In this chapter, some concepts of IEEE 802.11 standard and adaptive antenna have been reviewed. The basic idea of channel reservation and channel contention is still used by our new protocol. We also reviewed some basic concepts related to adaptive antenna, including beamforming and known adaptive algorithms.

# Chapter 3

## DOA Estimation

### **3.1 Introduction**

In this chapter, we study important aspects related to the DOA error. In particular, we study the performance degradation caused by imperfect GPS position estimation error in the directional MAC protocols proposed by Pan *et. al* [10]. Then, we study the effect of different system parameters on the accuracy of ESPRIT DOA estimation algorithm.

### **3.2 Effect of GPS Position Estimation Error**

A common assumption in almost all previously proposed DMAC is that perfect node position information is available. Typically, each ad hoc station is assumed to be equipped with a GPS to determine its position. In general, it was noticed that increasing the number of antennas can play an important role in improving the total system throughput for these directional MAC protocols when perfect position information is

available. Although GPS has been designed to be as nearly accurate as possible, there are still estimation errors that can cause a deviation of up to  $\pm(50 - 100)$  meters from the actual GPS receiver position. These errors are due to several factors such as atmospheric conditions, ephemeris errors, selective availability, and multipath [37]. In this section, we investigate the effect of inaccurate node position estimation on the throughput of these protocols. Our results show that, in contrary to the ideal case, as the inaccuracy of the position estimate increases, the system throughput decreases dramatically with the number of antennas and hence the conclusions drawn from previous work on directional MAC protocols should be interpreted with care.

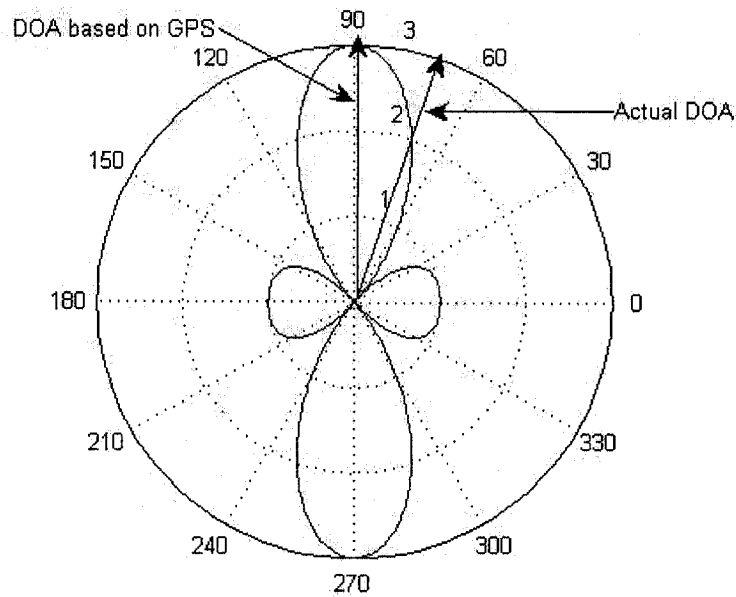


**Figure 3.1 Beampattern of Directional Antenna, NOE=3.**

Consider the antenna beampattern of a transmitter node shown in Figure 3.1. The main lobe is supposed to be pointing at the intended receiver (at angle 70 degrees). However, due to error in DOA estimation, the main lobe is focused towards another node

at angle 90 degrees. From Figure 3.1, it is clear that the signal level is degraded. Lower transmitted signal amplitude means the signal strength received at the intended receiver is also degraded and hence the bit error rate (BER) increases. The situation can become even more dramatic if the null part of beam faces the direction of intended receiver. Another problem may also arise if the wrong direction of the beampattern interrupts an ongoing transmission between two other nodes.

As will be shown by our simulations, in contrary to the ideal case, as the position estimation error increases, the system throughput dramatically decreases with the number of antennas. This can be intuitively explained by noting that the beampattern becomes narrower as the NOE increases and hence the effect of DOA estimation error becomes more dramatic.

### **3.3 *Effect of inaccurate GPS Position Estimation***

In this section, we focus on the directional MAC protocol proposed in [10] since it has proved to offer a significant throughput improvement relative to other existing protocols. Our findings, however, still apply to other directional MAC proposals.

To discuss how the inaccurate GPS information affects the whole system capacity, we consider a simple ad hoc network consisting of 10 nodes randomly scattered in a square area of 200 meters by 200 meters. Each station randomly moves in this network resulting in a different (random) network topology at different simulation times. Furthermore, half of stations act as transmitters and the other half act as receivers during the 1 second simulation period. We set channel rate = 1Mbps and every transmitter is assumed to be

fully loaded which means that every transmitter always has data to be transmitted. We assume that all mobile nodes are equipped with the same NOE. Figure 3.2 shows the average throughput over additive white Gaussian noise (AWGN) channel for uniformly distributed DOA error (on the x-axis, if DOA error = 5 degrees, this means that the error is uniformly distributed between -5, and +5 degrees).

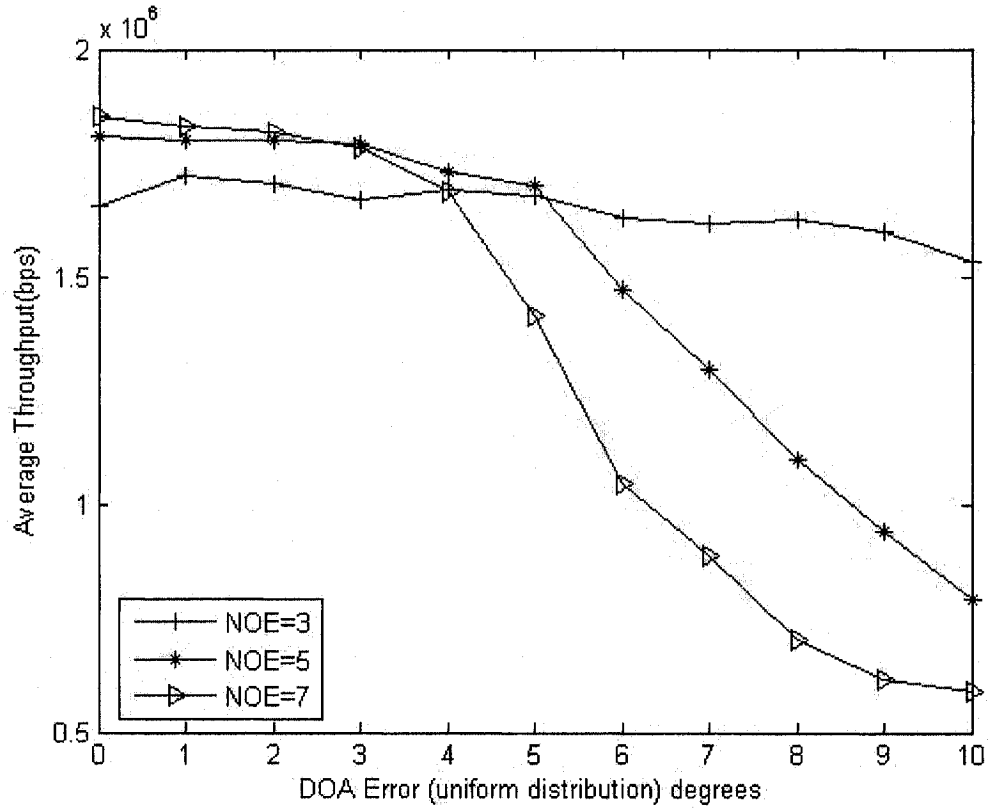


**Figure 3.2 Average throughput for different NOE versus DOA Error (uniform distribution) in AWGN channel, (10 nodes, 30 random topologies), SNR=20dB.**

As shown in Figure 3.2, when the DOA error is smaller than 3 degrees, the average throughput does not vary greatly with the NOE. It is also clear that when the DOA error increases above 4 degrees, the system capacity degrades dramatically for NOE=5, and 7. On the other hand, the throughput remains almost unchanged for NOE = 3.

The results presented in Figure 3.3 assume that the DOA error follows a Gaussian distribution with zero mean (the x-axis shows the variance). Similar conclusions follow by analyzing Figure 3.3.

Figures 3.4 and 3.5 show the corresponding results when we increase the number of mobile nodes to 30. Again, it is clear that when perfect position estimation information is available, increasing the NOE improves the system performance. On the other hand, the system performance degrades dramatically if this assumption does not hold.

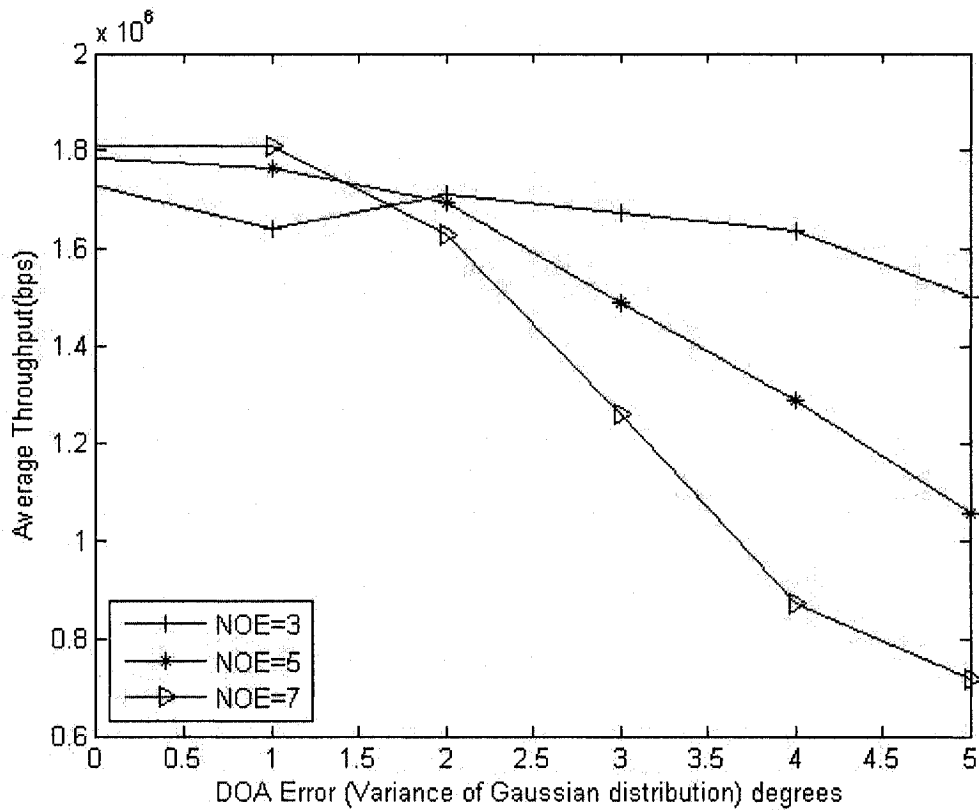


**Figure 3.3 Average throughput for different NOE versus DOA Error (Gaussian distribution) in AWGN channel, (10 stations, 30 random topologies), SNR=20dB.**

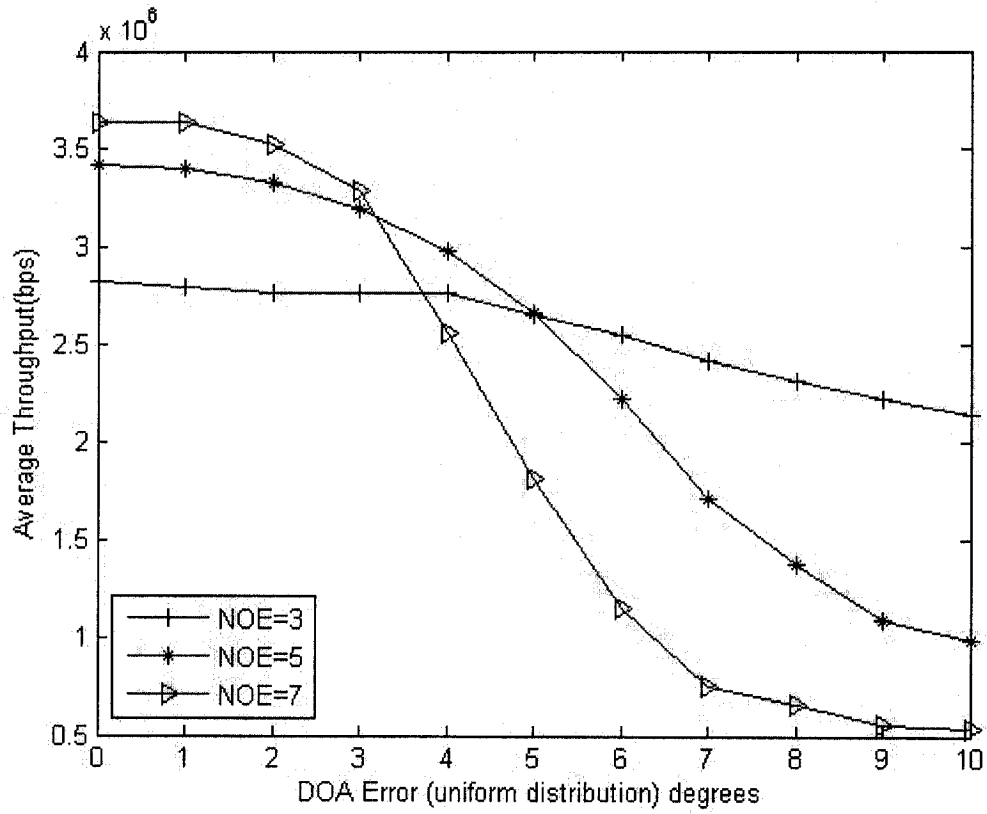


**Figure 3.4 Average throughput for different NOE versus DOA Error (uniform distribution) in AWGN channel, (30 stations, 30 random topologies), SNR=20dB.**

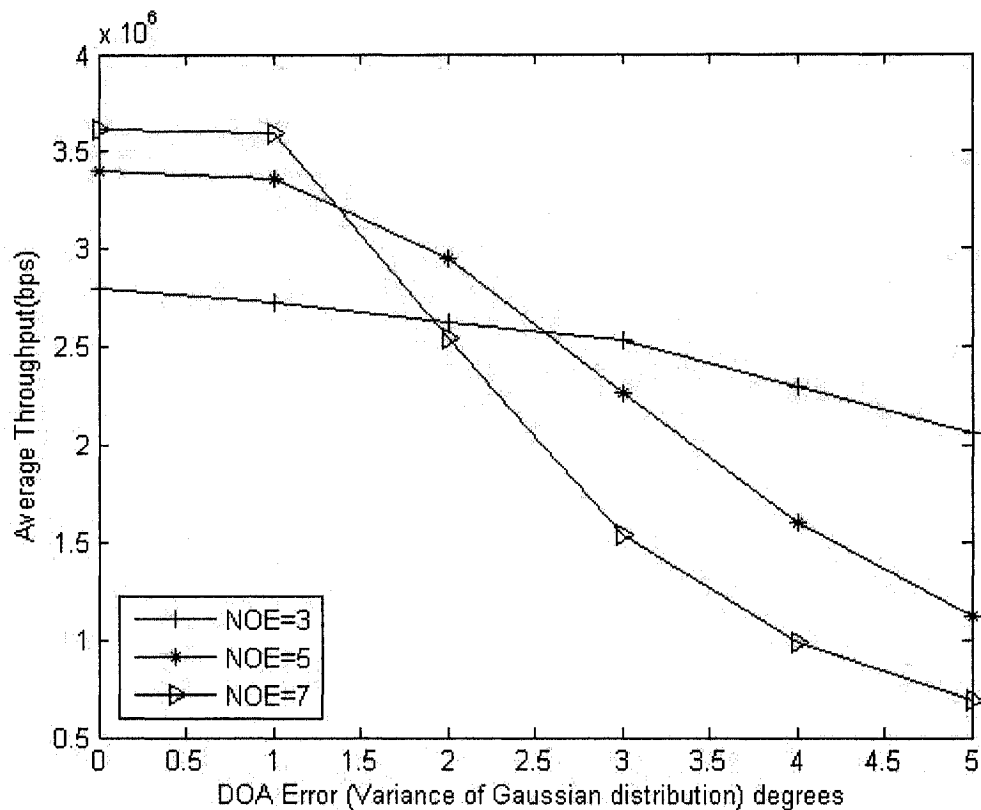


**Figure 3.5 Average throughput at different NOE versus DOA Error (Gaussian distribution) in AWGN channel, (30 stations, 30 random topologies), SNR=20dB.**

### 3.4 Accuracy of the ESPRIT estimation algorithm

In this section, we investigate the accuracy of the ESPRIT algorithm as a function of the system parameters, which include the number of array elements, the number of mobile users, angle of arrival, and SNR. Our simulation results show that the ESPRIT DOA estimation algorithm can provide enough accuracy for DMAC protocols.

Figure 3.6 shows the estimated mean DOA error,  $E(|e|)$ , generated with 3, 5 and 7 array elements. Furthermore, the signal of intention (SOI) is set to 30 degrees, and the number of samples (NOS) is set to 100. It is evident that using more elements improves

the accuracy of the ESPRIT algorithm. This is achieved, however, at the expense of increased computational complexity and added hardware. The simulation range for the number of interfering users and the number of antenna elements is justified by noting that the number of simultaneous signals that the antenna array can estimate must be less than number of elements in the antenna array.

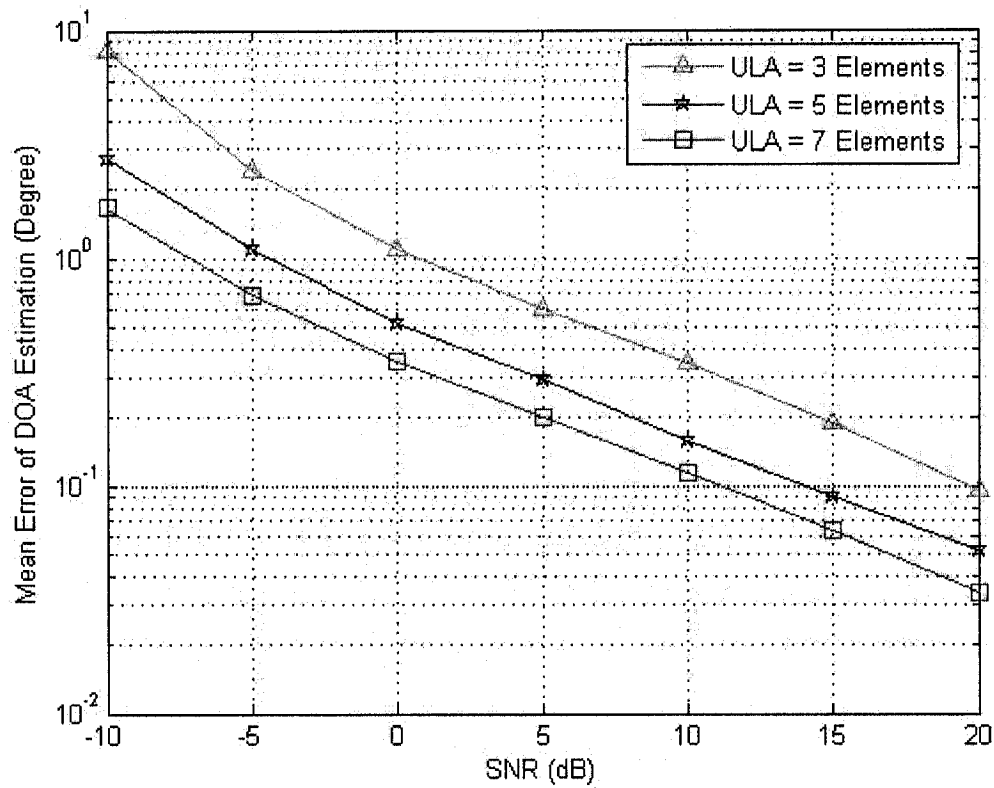


**Figure 3.6** The effect of SNR versus estimated mean error (SOI=30 degree, NOS=100,  $d = \lambda/2$ ).

When we change the number of active users, the number of signals received at the antenna array also changes. Throughout our simulations, we assume that all active users use the channel simultaneously. As shown in Figure 3.7, the performance of the algorithm degrades when the number of mobile users increases. In the simulation, the

SOI is set to 30 degrees and the angle of the interfering users are uniformly distributed in [0 180] degrees.

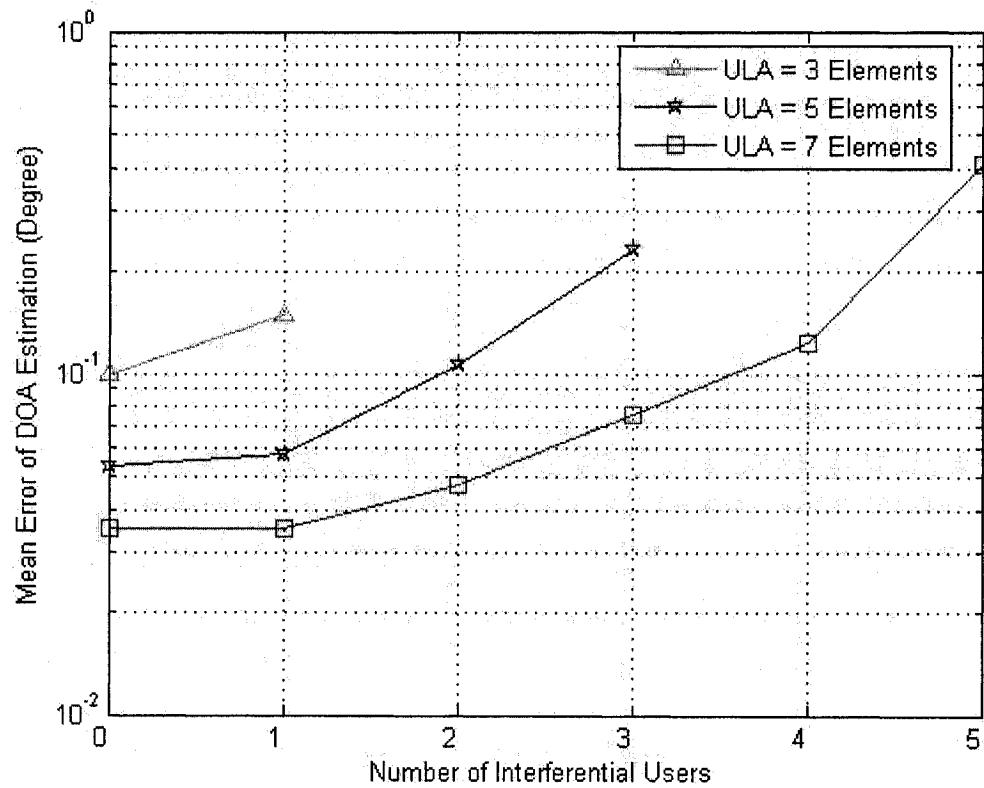


**Figure 3.7 The effect of number of mobile user versus estimated mean error (SOI=30 degree, SNR=20dB, NOS=100,  $d = \lambda/2$ ).**

As mentioned above, the maximum number of DOAs that a ULA can estimate must be less than the number of elements in the antenna array. For example, if the NOE is equal to 5, the maximum number of interfering users that can be nulled is 3 (1 SOI, and 3 interference signals).

The number of samples used to generate a realistic signal model is a key factor in the realization of practical DOA estimation system. Figure 3.8 shows the mean error of DOA estimation versus different number of samples. It is evident that increasing NOS leads to

a smaller estimation error. However, higher accuracy is achieved at the cost of longer processing time.

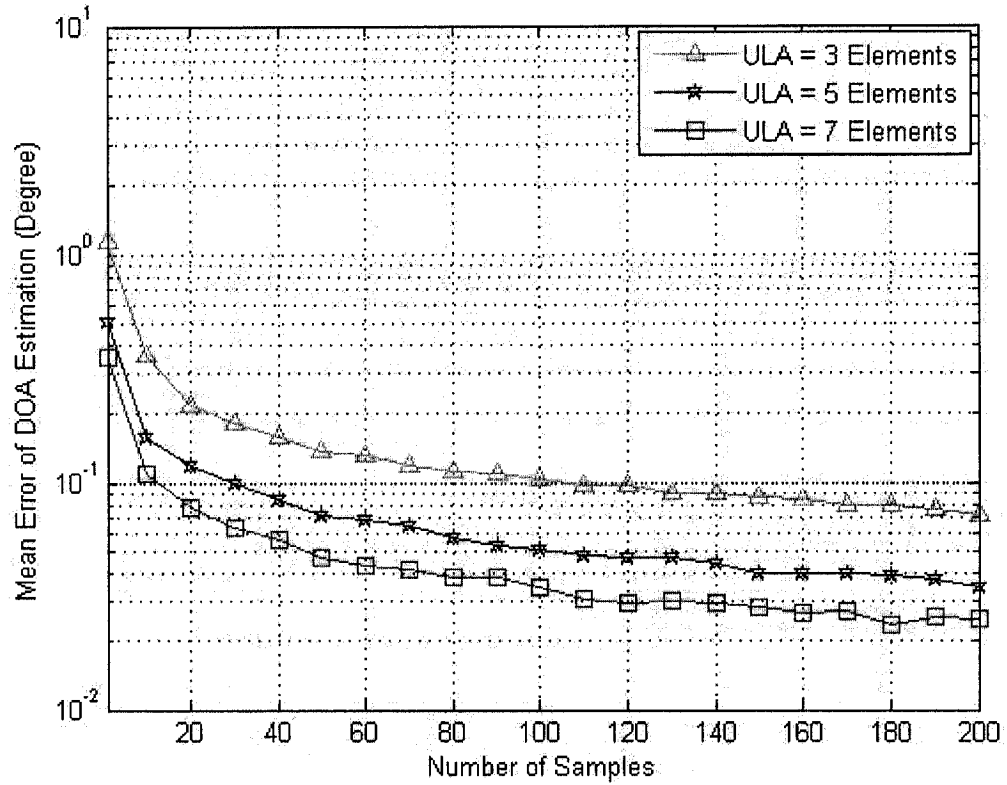


**Figure 3.8 Number of samples versus estimated mean error (SOI=30 degree, SNR=20dB,  $d = \lambda/2$ ).**

Figure 3.9 provides the simulation results when the arrival angle is changed. It is clear that the estimation accuracy degrades dramatically when the angle of arrival is in the 0 degree or 180 degrees neighborhoods.

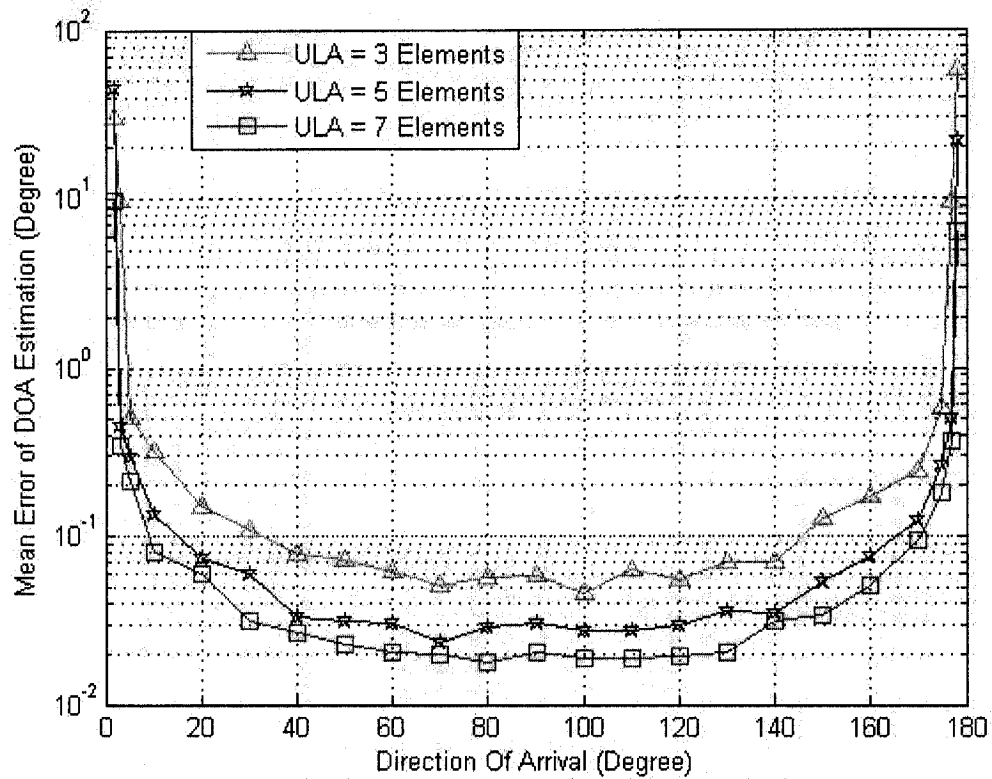


Figure 3.9 The direction of arrival versus the estimated mean error (SOI=30 degree, SNR=20dB, NOS=100,  $d = \lambda/2$ ).

### 3.5 Summary

In this chapter, we investigated the performance of one recently proposed DMAC protocol with inaccurate GPS position estimation. We also presented some simulation results to illustrate the accuracy of the ESPRIT DOA estimation algorithms using antenna array.

# Chapter 4

## Protocol Description

### *4.1 Introduction*

In this chapter, we present our new DMAC protocol. In section 4.2, the four basic steps of our protocol will be presented by considering different network scenarios. Finally in section 4.3, we provide a geometrical argument in order to determine the number of antenna elements required by our protocol.

### *4.2 Protocol description*

Our proposed MAC protocol is a two-channel two-mode (omni and direction) DMAC protocol. In channel one, all packets are sent in omni mode. In channel two, all packets are sent in directional mode. The mobile nodes are assumed to be equipped with directional antennas.

In our proposed protocol, we use two different values for network allocation vector (NAV). The first is referred as omni-NAV (ONAV) which counts the period during which a node cannot use channel one to transmit packets (similar to function of NAV table in IEEE 802.11). The second one is a directional-NAV (DNAV) which counts the

period during which a node cannot use channel two in certain direction. Thus, the DNAV can be seen as a table that keeps track of the blocked directions and the corresponding durations toward which a node must not initiate a transmission. If a node wishes to send a directional packet in channel two, and this direction is blocked by DNAV table, then it needs to defer this transmission. However, a transmission intended towards other directions that are not blocked by DNAV table can still be initiated.

In order to illustrate this, consider the scenario shown in Figure 4.1. Assume that node A and B communicate with each other using directional antennas. Also assume that all nodes are in the radio range of each other.

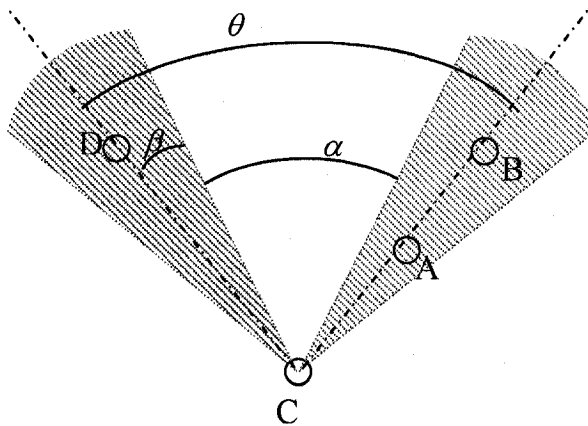


**Figure 4.1 An example of the function of the DNAV table.**

During the period of communications between node A and B, if node C has a packet to send to D, then it must check its DNAV table to see if it is safe to transmit in this direction. Since node C has already received a directional packet from node B only, it updates its DNAV table. Therefore, node C finds it is safe to transmit in the direction of

D. We assume that the directional beamwidth is  $2\beta$  degrees. Let  $\theta$  be the new initial transmission direction apart from the direction of ongoing transmission. Then  $\theta$  is given by

$$\theta = 2 \times \beta + \alpha \quad (4.1)$$

where  $\alpha$  is the angular separation of the range edges of the beamformers. If  $\alpha$  is negative, then the two beamformers might overlap. In our protocol, we must make sure that  $\alpha$  is greater than or equal to zero before any ongoing transmission can proceed.

To illustrate the basic steps in our new proposed MAC protocol, consider the scenario shown in Figure 4.2 which consists of 6 mobile nodes, A, B, C, D, E and F.

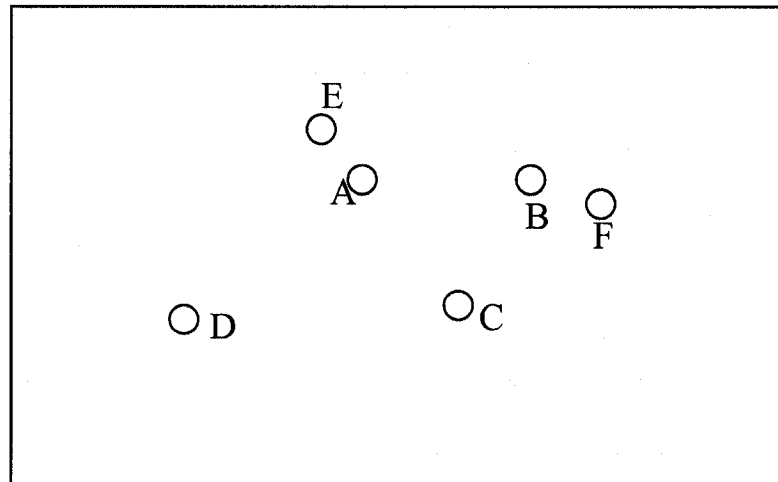


**Figure 4.2 6-node scenario.**

The nodes in our protocol can operate in two modes (i.e., omni-mode and directional mode). This scenario is designed to clarify the communication process between all possible neighboring pairs. In particular, it illustrates the communication process for the 3 types of neighboring pairs: (i) omni node, omni node, (ii) omni node, directional node, and (iii) directional node, directional node.

In the above scenarios, we consider nodes A and B as the transmitting pairs, nodes C and D as omni nodes, nodes E and F as directional nodes. We separate the whole process into four steps, which are “RTS transmission”, “RTS reception and CTS transmission”, “CTS reception and DATA transmission” and “DATA reception and ACK transmission”. In what follows, we describe the details of each one of these four steps.

- RTS transmission:

Assume that node A wishes to initiate a transmission with node B as shown in Figure 4.3. If channel one is sensed idle, node A sends an RTS frame to B in the omni mode using channel one. All mobile nodes remain in the omni mode when they are idle, listening to channel one. Thus node C, D, E, and F will update their ONAV. This stage is the same as in the IEEE 802.11.

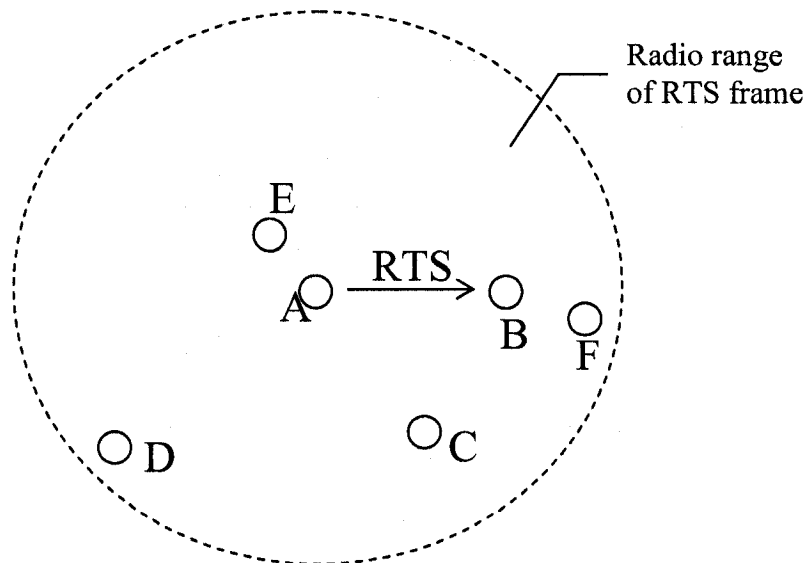


**Figure 4.3 RTS transmission stage.**

- RTS reception and CTS transmission:

In this step, all the mobile nodes determine the DOA of incoming signal using the ESPRIT DOA estimation algorithm. Having received the RTS from A, node B can determine the direction that it uses to send its CTS response. After checking its DNAV table, node B can also determine whether it is safe to use the direction of A in channel two. If it is safe, the physical layer at node B senses channel one for SIFS time slots. If channel one remains free during this interval, a CTS frame is transmitted using omnimode (OCTS) in channel one. At the same time of the OCTS transmission, node B sends another CTS using directional mode (DCTS) in channel two. As indicated in Figure 4.4, node A, C, E, F will receive the OCTS and update their ONAV table (similar to IEEE802.11). On the other hand, only nodes A and E will receive DCTS, and hence node E will consequently update its DNAV table.

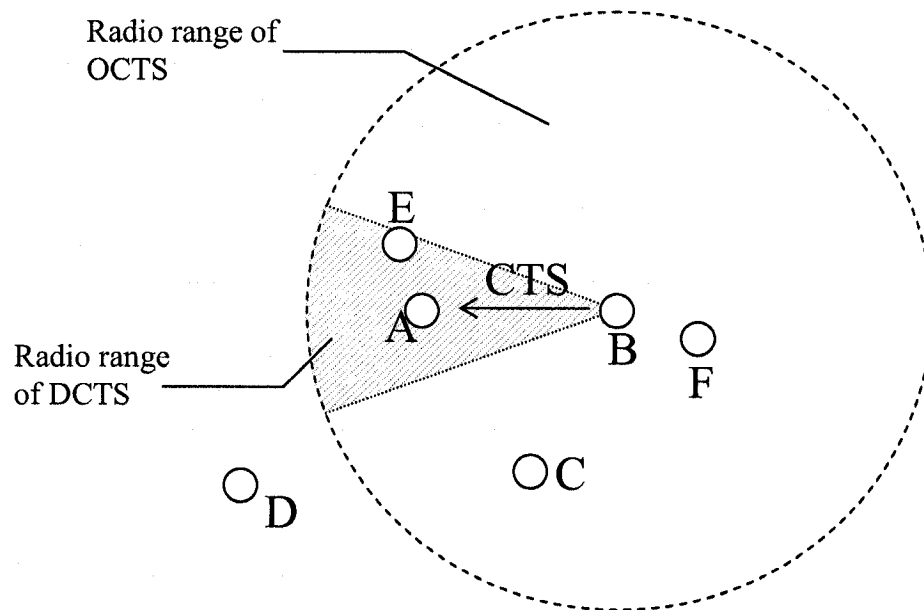


**Figure 4.4 CTS transmission stage.**

Compared to the IEEE 802.11, our proposed protocol uses a DCTS besides OCTS. The function of this DCTS is to update the DNAV table for all nodes which are located in the radio range of the ongoing transceiver's directional antenna in channel two. Hence these nodes will not try to send any signals that may interfere with ongoing transmissions. As shown in Figure 4.5, node E will update its DNAV table when it receives DCTS from B. The shadow part is the blocked range in E's DNAV table, which means that node E cannot initiate any transmission that is directed to this blocked area. For example, node E cannot set up any DATA transmission to node F during the period of DATA transmission between nodes A and B. Once node A and B finish the handshake stage in channel one, they start transmitting their DATA frames over channel two using the directional antenna mode. In particular, similar to the one it used to send DCTS, node B will use the directional beampattern to receive data from node A, and keep the null part in other directions to eliminate any potential interference.

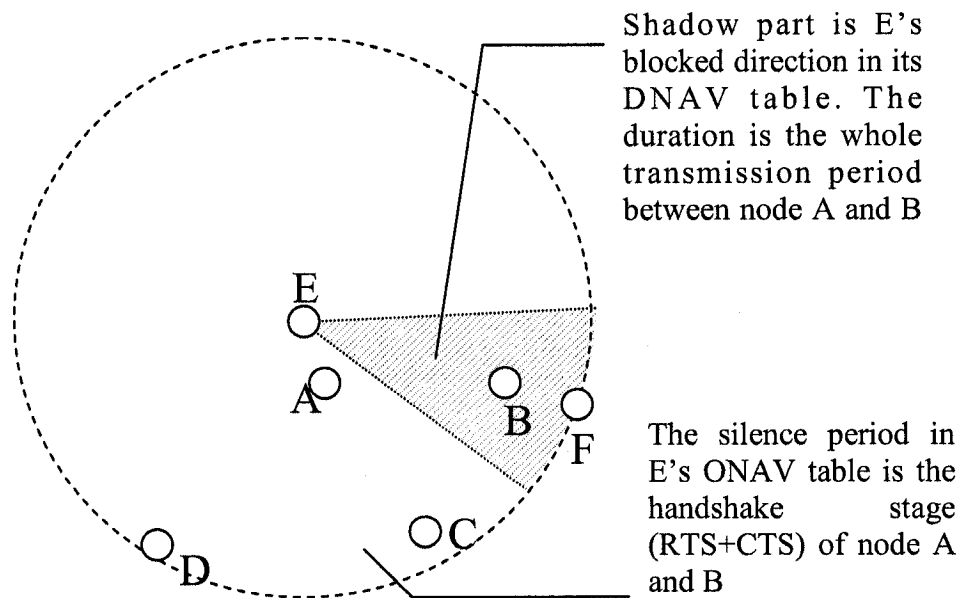


**Figure 4.5 The blocked direction in the DNAV table.**

- CTS reception and DATA transmission:

The sender (node A) waits for the CTS using the omni mode. If no feedback arrives within the timeout duration, node A will retransmit a new RTS packet. When node A receives the CTS, knowing the direction of receiver from DOA estimation, it initiates the DATA transmission using the directional mode over channel two provided that this direction passes the examination of its DNAV table. The antenna beamforming is demonstrated in Figure 4.6. Since nodes A and B have known the direction of each other, node A can send DATA over channel two using the directional mode. Similarly, node B can point its directional antenna to node A so that the interference from other directions may not affect the ongoing DATA transmission.

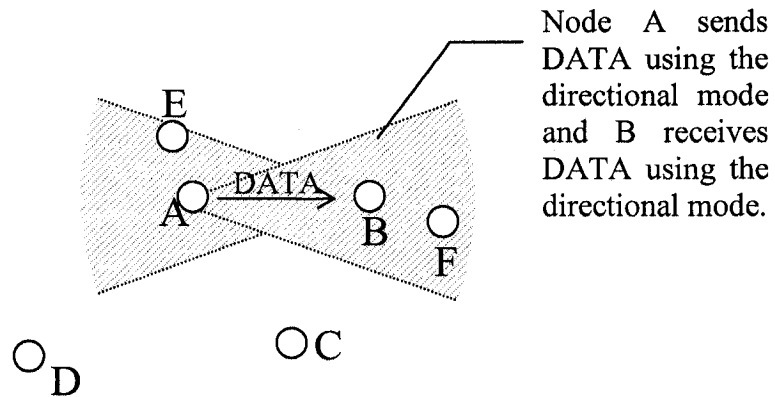


**Figure 4.6 DATA transmission stage.**

- DATA reception and ACK transmission:

On receiving the DATA successfully, node B sends an ACK using the directional mode over channel two. The antenna beamforming in this case is demonstrated in Figure 4.7. Node A will then point its directional antenna to node B to receive ACK. Due to the use of directional antennas, new transmissions can be set up in the vicinity of node A or B if it is not covered by the range of the directional antenna. As a result, the whole system capacity will be dramatically increased compared to the original IEEE 802.11 protocol. In summary, the transmission process will occupy channel one in the stage of RTS+OCTS, and channel two in the DCTS+DATA+ACK stage.

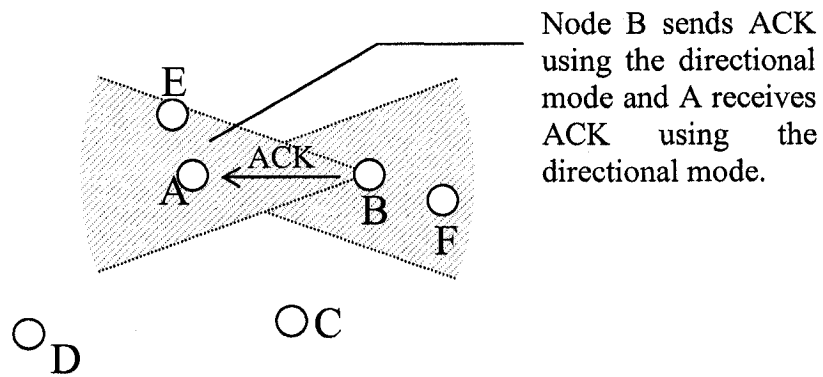


**Figure 4.7 ACK transmission stage.**

Now, we consider the new transmission if there is an ongoing transmission in its vicinity. All nodes, if they have packets to send, can contend over channel one after sensing channel one free for SIFS time slots. Consider the mobile nodes C and D in Figure 4.8. The ongoing DATA transmission of nodes A and B will not affect their transmission. Thus both nodes C and D can initiate transmission during the period of DATA transmission of A and B. This is simply because none of them receive packets in channel two (i.e. DCTS or DATA). On the other hand, the situation is different for node E and F. Node E is able to hear the DCTS form node B as discussed above. Thus node E will update its DNAV table in the direction to B. Also node F can hear the DATA packets form A so that node F will not initiate any transmission in the direction of node A.

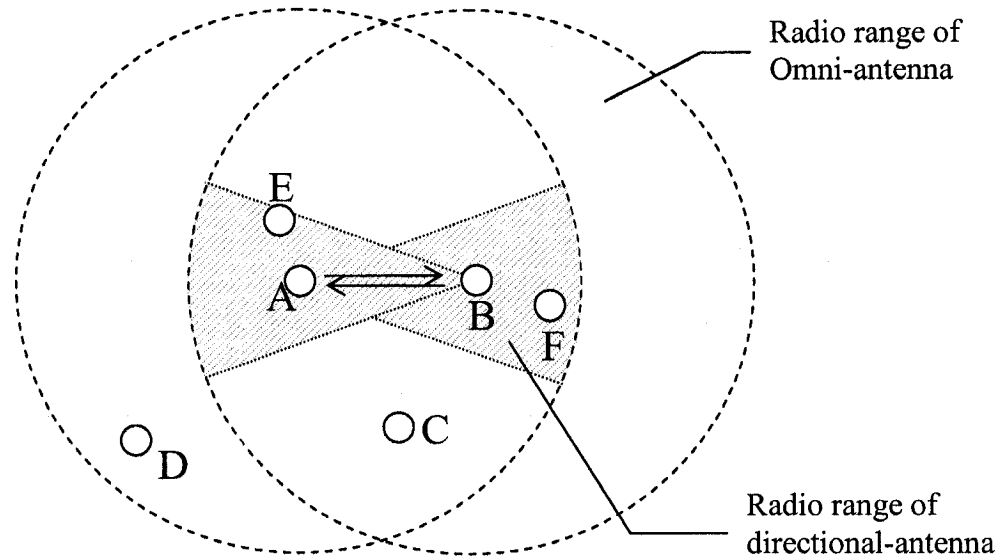


**Figure 4.8 Antenna beamforming for an ongoing transmission (Shadow part is the radio range of the directional antenna).**

As shown in Figure 4.8, node E can initiate a transmission to node D even though both of them are in the omni range of A. This type of transmission is impossible in the IEEE 802.11. Node E can also transmit data to node C even if the transmission direction is pointing to node A. This is forbidden in most of other DMAC protocols because node A is part of an ongoing transmission. Obviously, node E cannot transmit data to node F because F is in the blocked range of E (given in its DNAV table). Another difference between our protocol and other DMAC protocols (e.g., [11] [12]) is that we also take interference into consideration when forming the antenna beampattern. For example, if node E initiates a transmission to D, node E will take the direction of B in DNAV table as an unintentional direction when it forms its antenna weights. In this case, the antenna beampattern of node E will eliminate the interference part that points to B.

Figure 4.9 summarizes the above steps. *Others-free* refers to all neighbors of the transceiver that can freely use channel two for their DATA transmission. *Others-blocked* refers to the transceiver's neighbors whose intended transmission is blocked by their DNAV tables.

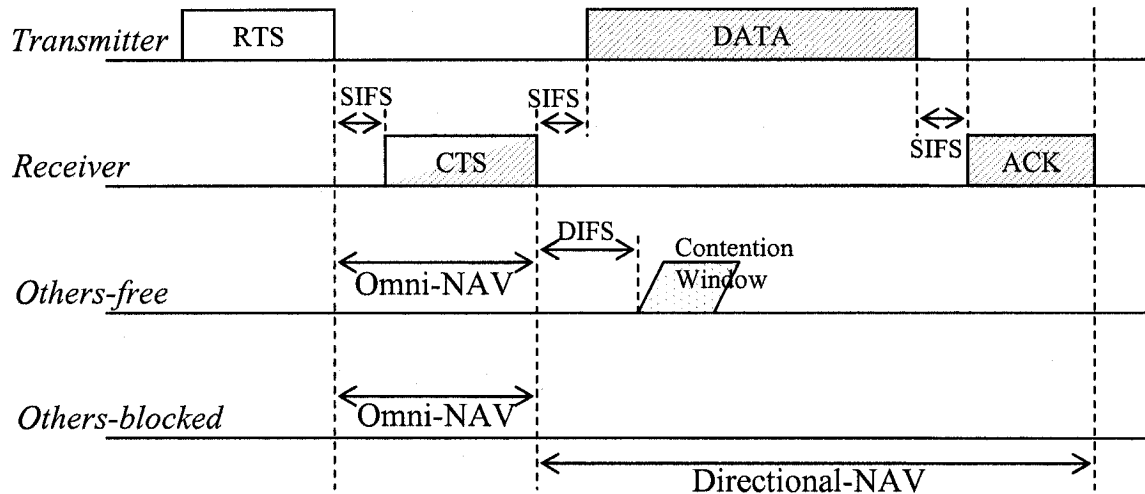


**Figure 4.9** Transmission process for the new MAC protocol

Figure 4.10 illustrates a 4-node scenario that is different from the scenario presented in Figures 4.2-4.8. In Figure 4.10, the 4 mobile nodes A, B, C and D are assumed to be distributed on a straight line from left to right, with a separation of 100 meters between nodes. Furthermore, the radio range of each antenna is also 100 meter. That means every station can communicate with its nearest neighbors only (e.g. node A transmits to node B, and node C transmits to node D).

As shown in Figure 4.10, when node B receives the RTS frame from node A, it will send OCTS and DCTS at the same time after a SIFS period. While node A will receive both OCTS and DCTS, node C will only receive OCTS. According to our protocol, node

C only needs to keep silent before B's OCTS finishes. After a DIFS period, node C can initiate its transmission to node D which is definitely not permitted by IEEE802.11.

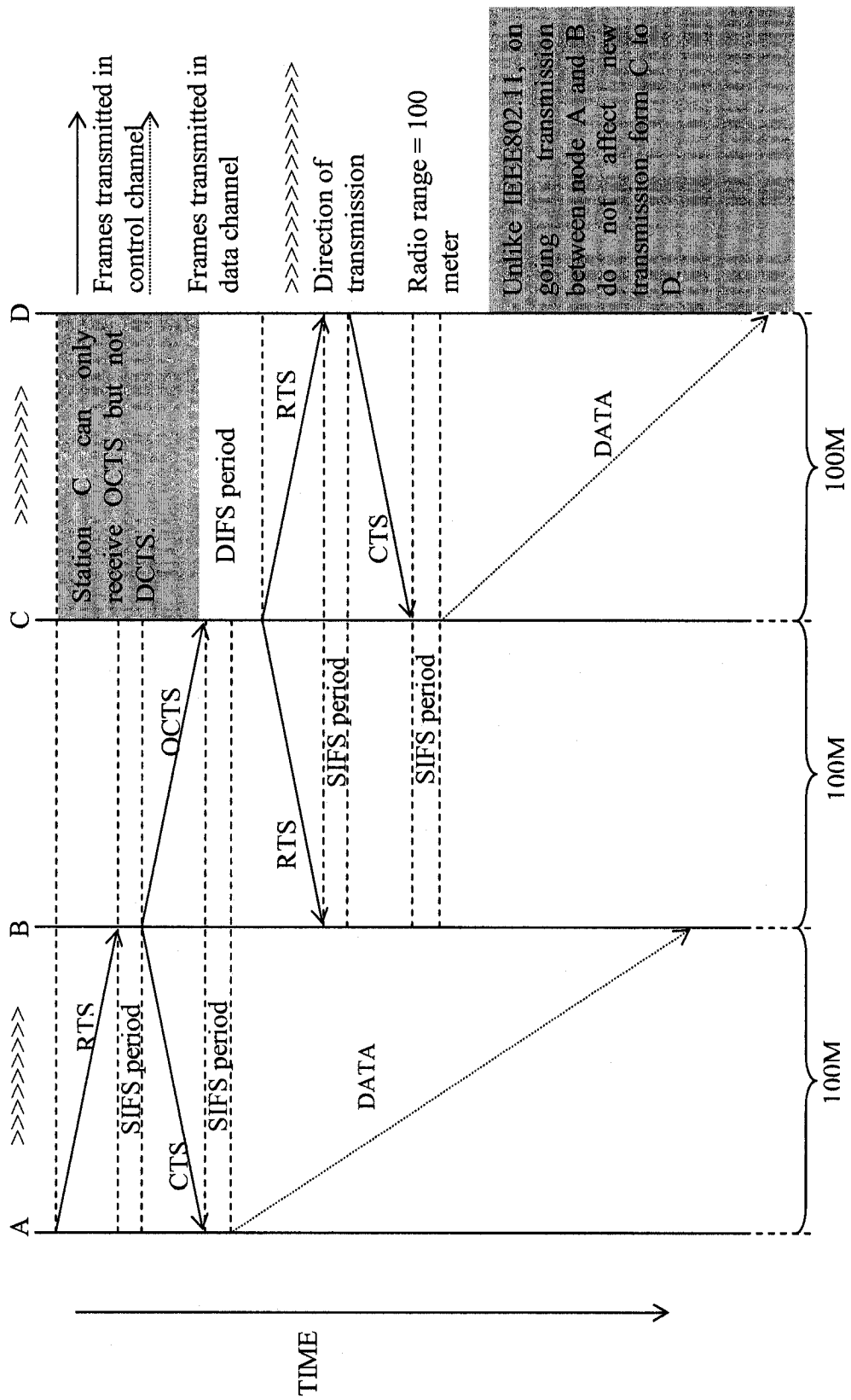
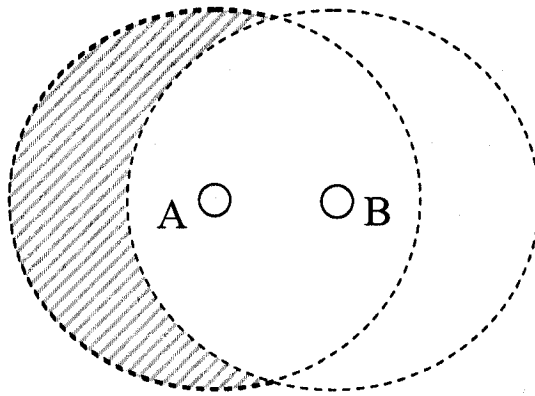


Figure 4.10 Timing diagram for a 4-station scenario.

### **4.3 Determining the number of antenna elements**

Although we can increase the number of antenna elements to reach a more accurate direction estimation and also eliminate more interferes in other directions, the dimension and cost of antenna array should be considered. On the other hand, as we mentioned in chapter 3, if an antenna array consists of  $M$  elements, then, the maximum number of signal directions that this adaptive antenna array can simultaneously estimate is  $M - 1$ . Since each mobile node can receive more than one signal at the same time, we should design our antenna array such that the NOE satisfies the above requirement. Since we use omni-mode RTS and CTS in the handshake process, and by noting that all DOA estimation are done only during this handshake stage, the number of signals that simultaneously reach a given mobile node cannot possibly be over than 5. The reason that mobile nodes cannot receive more than 5 signals will be illustrated below:

1) Consider the proposed scenario in Figure 4.11. As shown, node A needs to estimate the DOA of its neighbors' signals. We assume that node B sends its signal first. Then, node A will know the direction to B. Other nodes in the radio range of B will keep silent during this period because B has occupied the channel. Other neighbors of A can only use the shadow region in Figure 4.11 if they wish to send any signal during the period in which node B occupies the channel. Otherwise, they have to keep silent because the remaining region has been reserved by node B.



**Figure 4.11 Illustration of simultaneous estimated signals (step 1).**

2) Since we would like to know the maximum number of neighbors that can send signals to A at the same time, we must make sure that the radio range of every station of A's neighbors occupies as little as possible of the radio range of A. This way, the number of mobile nodes in the radio range of A can reach its maximum. In Figure 4.12, node B is located just at the edge of A's range. We can see that the shadowed area is obviously larger than the corresponding shadow in Figure 4.11. Recall that we use the shadowed region to represent the free radio range that other new incoming nodes can use to send their signals and can be heard by node A. It is clear that the scenario in Figure 4.12 gives other neighbors more free space to send their signals to A.

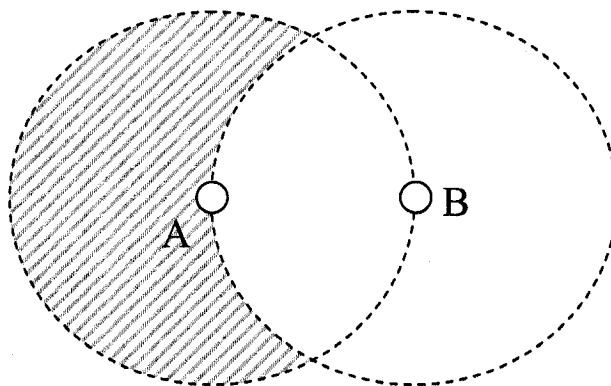


**Figure 4.12 Illustration of simultaneous estimated signals (step 2).**

3) In Figure 4.13, a new node, C, uses the free channel to send signals because it is in the range of A but not in the range of B. Note that node A can estimate the direction of B and C at the same time. The shadow area indicates the region that can be used by other neighboring nodes for signal transmission.

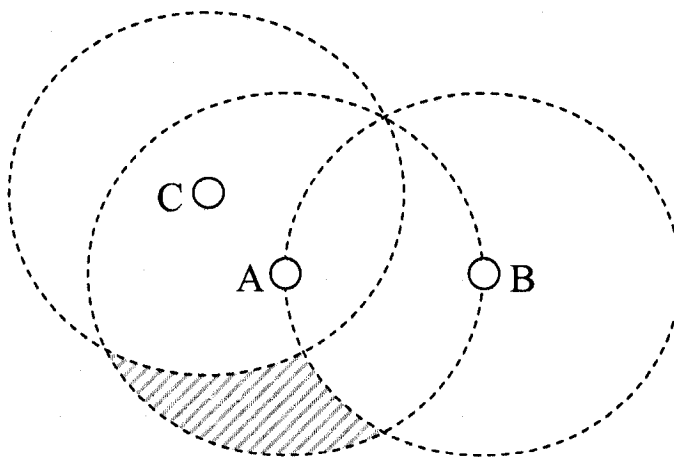


**Figure 4.13 Illustration of simultaneous estimated signals (step 3).**

4) As shown in Figure 4.14, if we wish to leave as large free space as possible for other neighbors, C must stay as close as possible to B but outside the radio range of B. That is to say, the length of BC should be a little bit longer than AB or AC in Figure 4.14. As a result, the angle of BAC is a little larger than 60 degree, and the shadow region can be occupied by other new nodes.

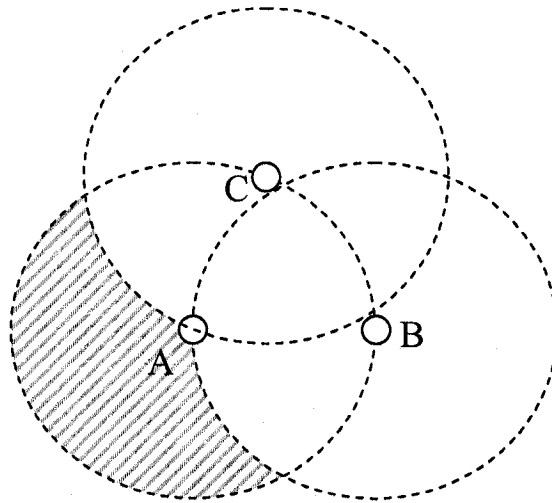


**Figure 4.14 Illustration of simultaneous estimated signals (step 4).**

By repeating the above argument, we can easily deduce that the maximum numbers of A's non interfering neighbors is 5. As shown in Figure 4.15, neighbors of A will be outside the radio range of each other but in the radio range of A.

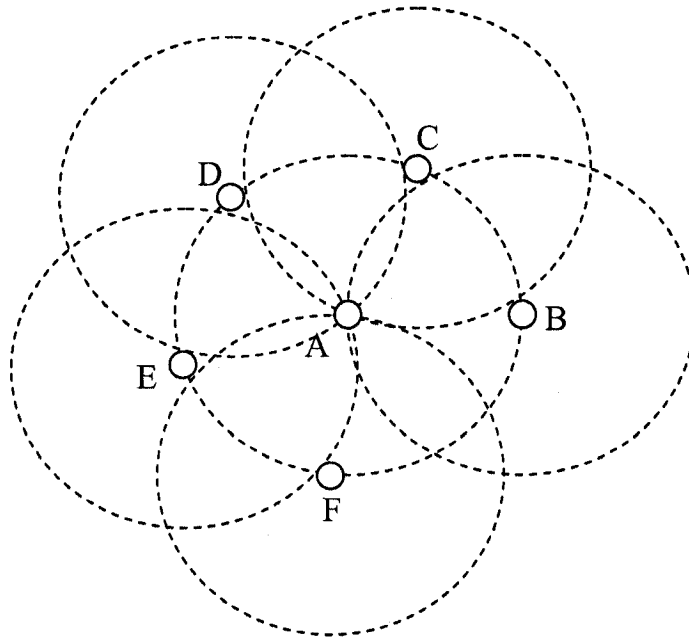


**Figure 4.15 Illustration of simultaneous estimated signals (step 5).**

#### **4.4 Summary**

In this chapter, we provided a detailed description of our propose protocol. We also proved that the NOE required by our DOA estimation algorithm must be at least 6. Based on the description provided in this chapter, one can think of our protocol as an enhanced version of Pan et. al [10] protocol. Our modifications allow us to avoid the reliance on GPS information and hence make our protocol suitable for indoor environments. These modifications also avoid the dramatic degradation in throughput associated with inaccurate GPS position estimation.

# Chapter 5

## Simulation Results

### *5.1 Introduction*

The simulation results presented in this chapter demonstrate the dramatic increase in the system capacity achieved by using our proposed 2-channel 2-mode DMAC protocol. In section 5.2, the simulation model is depicted. In section 5.3 and section 5.4, our simulation results using random and specified scenarios are presented.

### *5.2 System Model*

#### **5.2.1 Topology and Parameters**

Throughout the first part of our simulation and in order to examine the efficiency of our new MAC protocol, we consider a scenario which consists of 10 nodes randomly scattered in a 200 meters  $\times$  200 meters area. This topology is shown in Figure 5.1. We also assume that half of the nodes act as transmitters if their buffers have data. On the other hand, the other half act as receivers that receive the data sent by their corresponding transmitters. We fix the combinations of transceivers during the period of our simulation

as follows: node 1 is transmitting to node 6, node 2 to node 7, node 3 to node 8, node 4 to node 9, and node 5 to node 10. A snapshot of this system topology is shown in Figure 5.1.

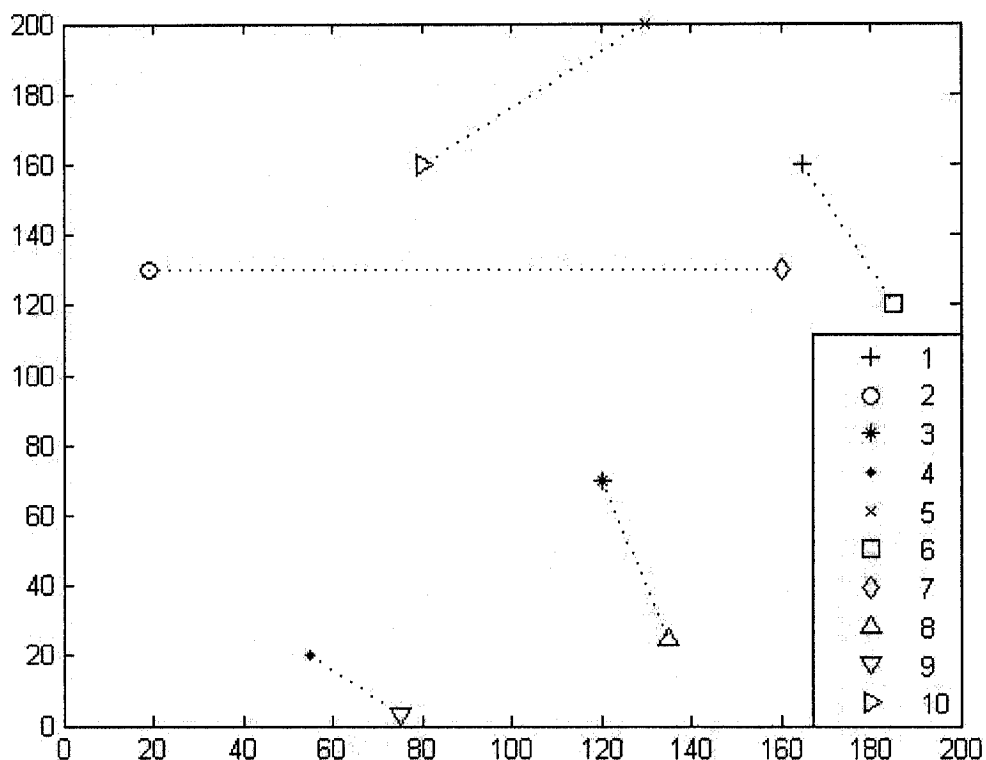


**Figure 5.1 Snapshot of a 10-station scenario with random configuration.**

The transmission range of the antennas in both modes (i.e., omni and directional modes) is fixed to 100 meters. The total throughput is average throughput from all node. That is the total throughput = frame length x number of frames transmitted successfully per second. The control frames, such as RTS/CTS/ACK, are not included in the throughput calculation. The simulation time is 1 second, and the channel rate is set to 1 Mbps with data frame length = 4,000 bits. All simulations are performed for both AWGN and Ricean fading channel. We also compare the performance of our proposed protocol

with the IEEE 802.11 protocol. The bit-error-rate (BER) threshold is set to  $10^{-5}$  which is used as a criteria to determine whether the received data frame is acceptable or not. If the BER is larger than  $10^{-5}$ , we consider it as a failed packet and do not count it into the total throughput.

Since the main focus of this work is on the performance of the proposed protocol using adaptive antennas, details regarding how data packets are handed over from upper layers are not studied in this thesis. At the beginning of the simulation, all data frames from upper layers are stored in the buffers of the mobile node. To simplify the simulation, similar to [10], we employ a simple single-hop routing protocol to solve the out of range problem. In this routing protocol, if the destination node is out the radio range of the source node, the transmission can only take place through a single hop (i.e., only one transceiver acts as router in the path from transmitter to receiver). Note that, one can employ more efficient routing protocols to solve the out-of-range problem. However, here we chose to use such a simple routing protocol to simplify the simulation. To be fair, all channel parameters are set the same as in IEEE802.11.

Later, we increase the number of nodes to 30 to illustrate the capacity gain in heavily loaded scenarios. We randomly generate the system topology at every simulation period. That is to say, every node will be randomly located in space.

### **5.2.2 Communication Channels**

In order to fully examine the proposed protocol in a realistic wireless channel model, in addition to the AWGN channel, we also simulate our protocol over fading channels. The behavior of a typical mobile wireless channel is considerably more complex than that of an AWGN channel. Besides the thermal noise at the receiver frontend (which is

modeled by AWGN), channel fading is the most direct impairment in a typical wireless channel.

Fading is a common phenomenon in mobile communication channels caused by the interference between two or more versions of the transmitted signals which arrive at the receiver at slightly different times. The resultant received signal can vary widely in amplitude and phase, depending on various factors such as the intensity, relative propagation time of the waves, bandwidth of the transmitted signal etc. The performance of a system (in terms of probability of error) can be severely degraded by fading. In this case, special techniques may be required to achieve satisfactory performance. The statistics describing the fading signal amplitude are frequently characterized as either Rayleigh or Ricean [31]. Rayleigh fading occurs when there is no line of sight (LOS) component present in the transmitted signal [34]. If there is a LOS component present, the fading follows a Ricean distribution [35]. Due to the frequent direct LOS path presented in ad-hoc communications, the most typical fading channel of indoor office building is Ricean channel where  $K=6$  [25] (The Ricean  $K$  factor used here denotes the ratio of LOS path power to the multipath components power). Therefore, it is often the case that Ricean fading is a good approximation of realistic ad-hoc networks. In Figure 5.2, we present the performance of QPSK system under different channel conditions. The impact of fading on the system performance is quite clear. For example, if we want to reach the minimum quality of service (QoS) requirement of  $10^{-5}$  BER, a SNR of 10 dB is needed in an AWGN channel. On the other hand, a SNR over 45 dB is needed if we wish to achieve the same system performance over a Rayleigh fading channel.

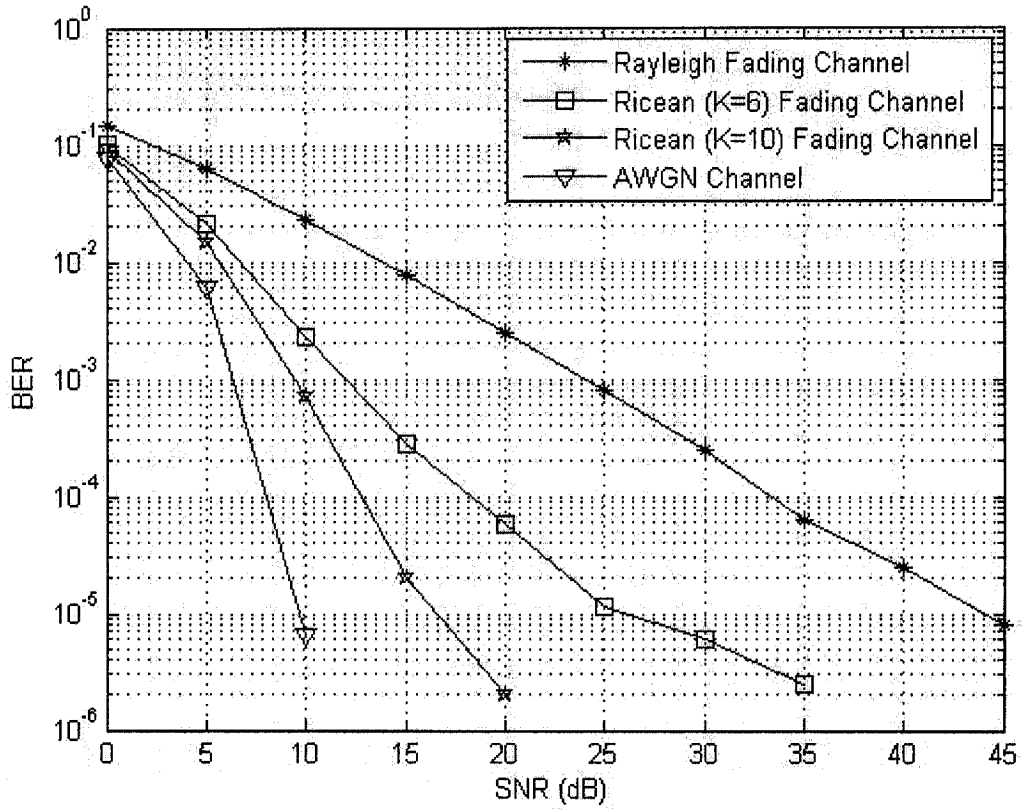


**Figure 5.2 QPSK signal BER for different channel conditions.**

The mathematical model for fading channels can be explained as follows, consider a transmitted signal  $S(t) = A\cos(2\pi f_c t)$  through multipath fading channel, where  $f_c$  is carrier frequency, and  $A$  is signal amplitude. If we do not consider the noise factor, the received signal can be expressed as:

$$r(t) = A \sum_{i=1}^N \alpha_i \cos(2\pi f_c t + \theta_i) \quad (5.1)$$

where the variables  $\alpha_i$  and  $\theta_i$  are the amplitude and the phase-shift of the  $i^{\text{th}}$  multipath signal component, respectively.  $N$  represents the total number of possible multipath components. Equation (5.1) can be rewritten as

$$r(t) = A\left[\sum_{i=1}^N \alpha_i \cos(\theta_i) \cos(2\pi f_c t) - \sum_{i=1}^N \alpha_i \sin(\theta_i) \sin(2\pi f_c t)\right]. \quad (5.2)$$

If we introduce two random processes  $G_1(t)$  and  $G_2(t)$ , where

$$G_1(t) = \sum_{i=1}^N \alpha_i \cos(\theta_i) \quad (5.3)$$

and

$$G_2(t) = \sum_{i=1}^N \alpha_i \sin(\theta_i). \quad (5.4)$$

Then, equation (5.2) can be expressed as

$$r(t) = A[G_1(t) \cos(2\pi f_c t) - G_2(t) \sin(2\pi f_c t)]. \quad (5.5)$$

when the received signal consists of a large number of scatters in the fading channel,  $G_1(t)$  and  $G_2(t)$  can be modeled, according to the central limit theorem [43], as zero mean Gaussian random variables. According to this, our simulation uses the sum of two quadrature random Gaussian noise signal as the flat Rayleigh fading channel coefficient. From the mathematical model of Ricean channel, the variance of the Gaussian random variable  $G_1(t)$  and  $G_2(t)$  is same as those for Rayleigh channel but its mean values are not zero.

### 5.3 System Performance Evaluation

For the randomly generated scenario, we assume 10 mobile nodes randomly scattered in 200 meter by 200 meter area and calculate the average system throughput for 30 randomly generated topologies. We study how the system performance varies with the

node load, SNR, and number of antenna elements. Finally, we examine the system performance in heavily loaded scenarios by increasing the number of mobile nodes.

### 5.3.1 System Performance under Different System Loads

In this case, we consider a network where all participating nodes are transmitting at the same load. Figure 5.3 shows the average throughput as the load varies from 0.1 Mbps to 1 Mbps. When the load per node is equal to 1 Mbps, the average throughput of our protocol is about 2.3Mbps which is more than the average throughput achieved by the IEEE 802.11 (1 Mbps). The reason for this improvement can be explained by noting that, in our protocol, several simultaneous transmissions can be allowed compared to IEEE 802.11 protocol, especially at high load situations.

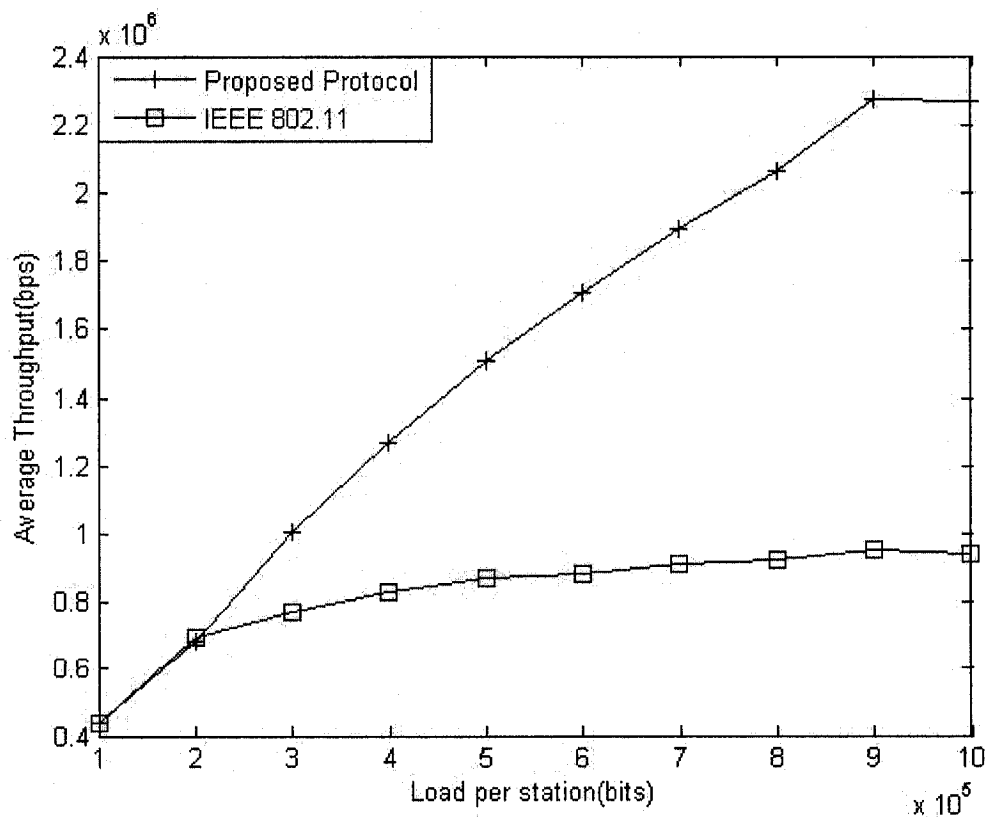


**Figure 5.3 Average throughput in AWGN channel (10 mobile nodes and 30 random topologies), SNR = 20dB, NOE= 6 (not applied to IEEE 802.11).**

On the other hand, the average throughput of both protocols are almost the same when the assigned load-per-node is light. The reason is that some nodes can finish their data transmission process when the simulation time is not over. That is to say, these nodes can leave the channel free to other waiting nodes for their data transmission or act as routers for other nodes which may be out of range of each other. As a result, irrespective of the MAC protocol they employ, all buffered data will be finished in time. On the other hand, when the load becomes heavy, those waiting nodes will not have enough time to finish their transmission.

### **5.3.2 System Performance under Different SNR**

Figure 5.4 shows how the SNR affects the performance of our protocol. When the SNR is lower than 5dB, both the IEEE802.11 and our protocol cannot transmit any data because even short packets, such as RTS/CTS, fail to be transmitted. Therefore, the transmitter must ensure that the system SNR is kept over 5 dB.

One should also remember that the SNR affects the accuracy of our DOA estimation algorithm which consequently affects the system throughput. From the results presented in chapter 3 and from Figure 5.4., it is clear that the SNR requirement of our DOA estimation algorithm is not so restrictive. As shown in Figure 3.6, the error range of DOA estimation is always lower than 1 degree when the SNR is larger than 5 dB. Compared to IEEE 802.11, it is clear that as SNR increases, our protocol offers a substantial throughput improvement. As shown in Figure 5.4, the IEEE 802.11 throughput is almost

zero at SNR=10 dB. On the other hand, the throughput of our protocol reaches over 2 Mbps over AWGN channel at the same SNR.

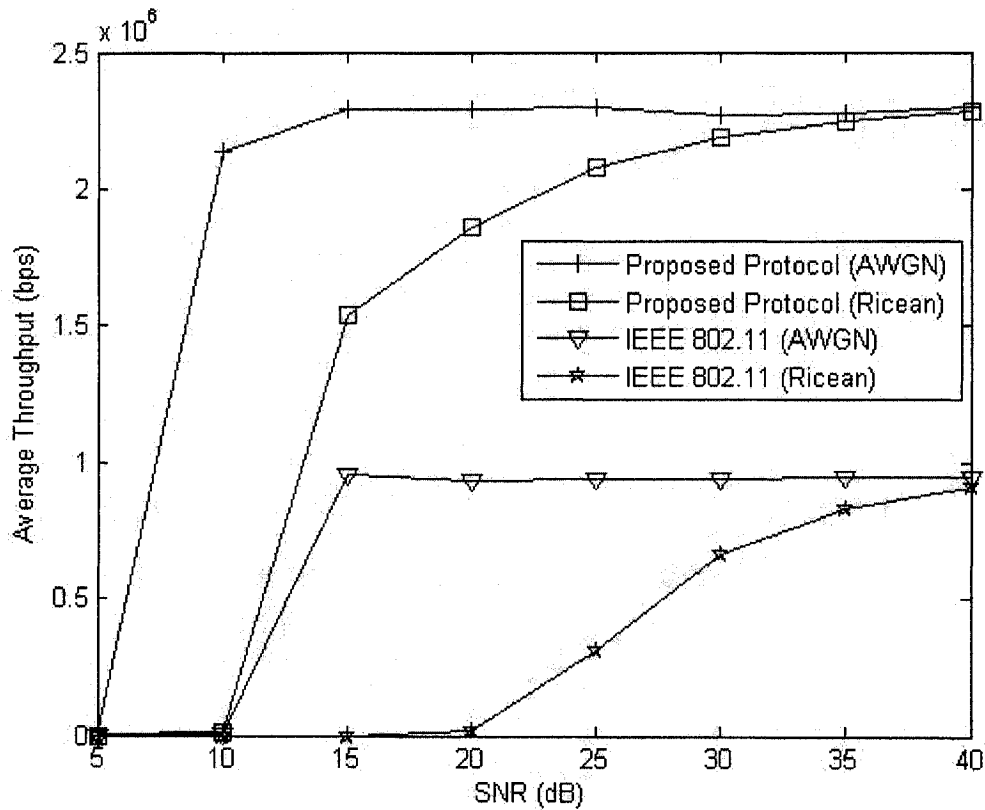


**Figure 5.4 Average throughput in AWGN and Ricean (K=6) fading channels (10 mobile nodes and 30 random topologies), Load\_per\_node=1Mbps, NOE= 6 (not applied to IEEE 802.11).**

Figure 5.4 also shows the performance of our MAC protocol over fading channels. Here, we assume a Ricean channel with K=6, which is a typical value for indoor office buildings [25]. For this channel, and for SNR=20 dB, the average throughput of the IEEE 802.11 is almost zero. On the other hand, our protocol reaches an average throughput of about 1.8 Mbps. The results clearly show how the use of directional antennas can alleviate the multipath fading effect.

One should also note that the performance reach the same level in Ricean and AWGN channel when the SNR=40 dB. This can be explained by noting that for such a high SNR, both channels satisfy our prescribed  $10^{-5}$  BER threshold.

### 5.3.3 System Performance under Different NOE

Figure 5.5, compares the performance of our protocol over a Ricean fading channel (SNR=30 dB) when using 6 and 7 antenna elements.

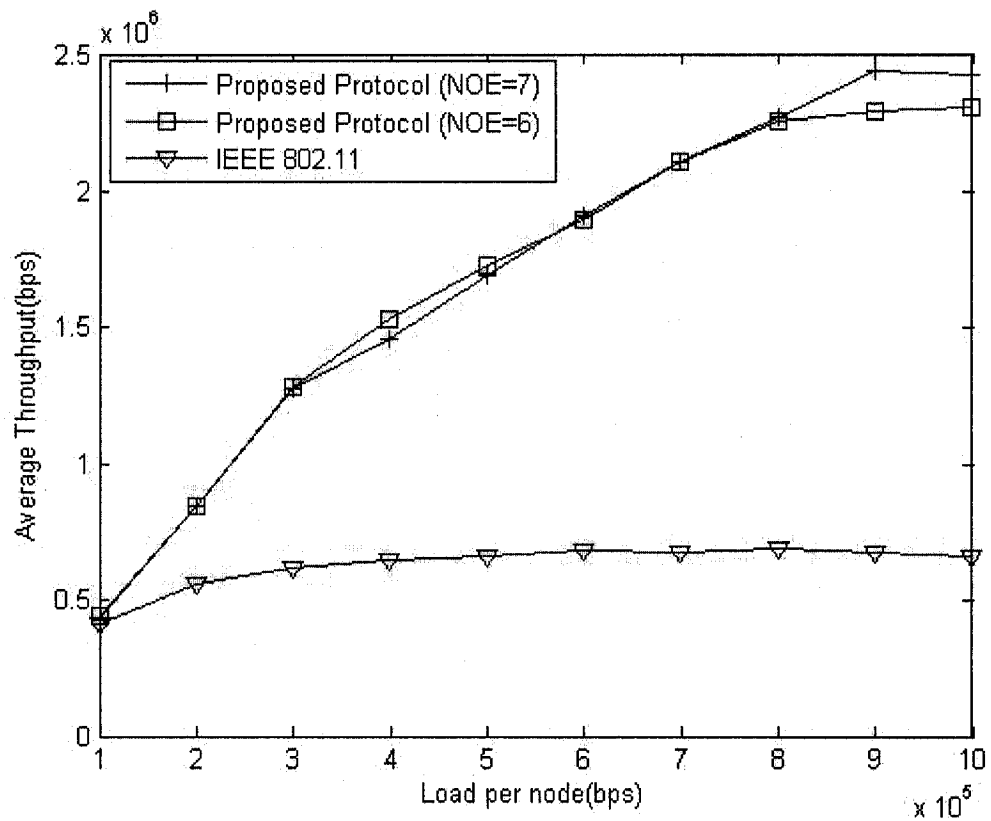
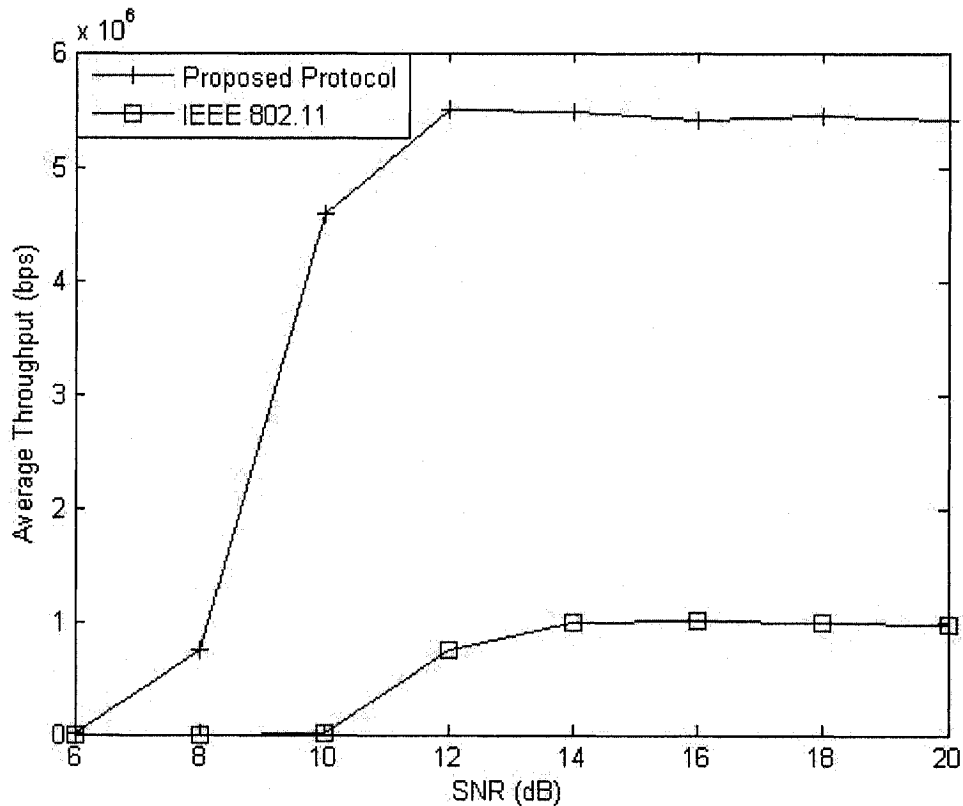


Figure 5.5 Average throughput in Ricean ( $K=6$ ) fading channel (10 mobile nodes and 30 random topologies), SNR=30dB.

Besides the throughput gain compared with IEEE 802.11, one should also note that the additional antenna element does not add any throughput improvement, i.e., 6 antenna elements are practically enough under light load conditions.

### 5.3.4 Number of users

In this section, we study the effect of increasing the number of nodes (i.e., increasing the node density) on the performance of our protocol. Instead of the 10 mobile nodes scenario, we consider 30 nodes. We still calculate the average throughput by averaging over 30 randomly generated topologies.



**Figure 5.6 Average throughput in AWGN channel (30 mobile nodes and 30 random topologies), Load\_per\_node=1Mbps, NOE= 6 (not applied to IEEE 802.11).**

Comparing Figure 5.6 and Figure 5.3 (the 10 mobile nodes), we can see that the maximum throughput of our protocol increases from around 2.3 Mbps to 5.5 Mbps. On the other hand, the maximum throughput of the IEEE802.11 only increases from around 0.9 Mbps to 1 Mbps. This can be explained by noting that as we increase the mobile node density, there will be more nodes contending for the channel at the same time. That is to say more nodes must stay silent due to the NAV period (in both our protocol and the IEEE 802.11). On the other hand, because of the advantage of directional antennas and the availability of two channels, our protocol does not require all nodes in the radio range to stay quiet during the DATA transmission process. Figure 5.7 shows similar results under varying system loads.

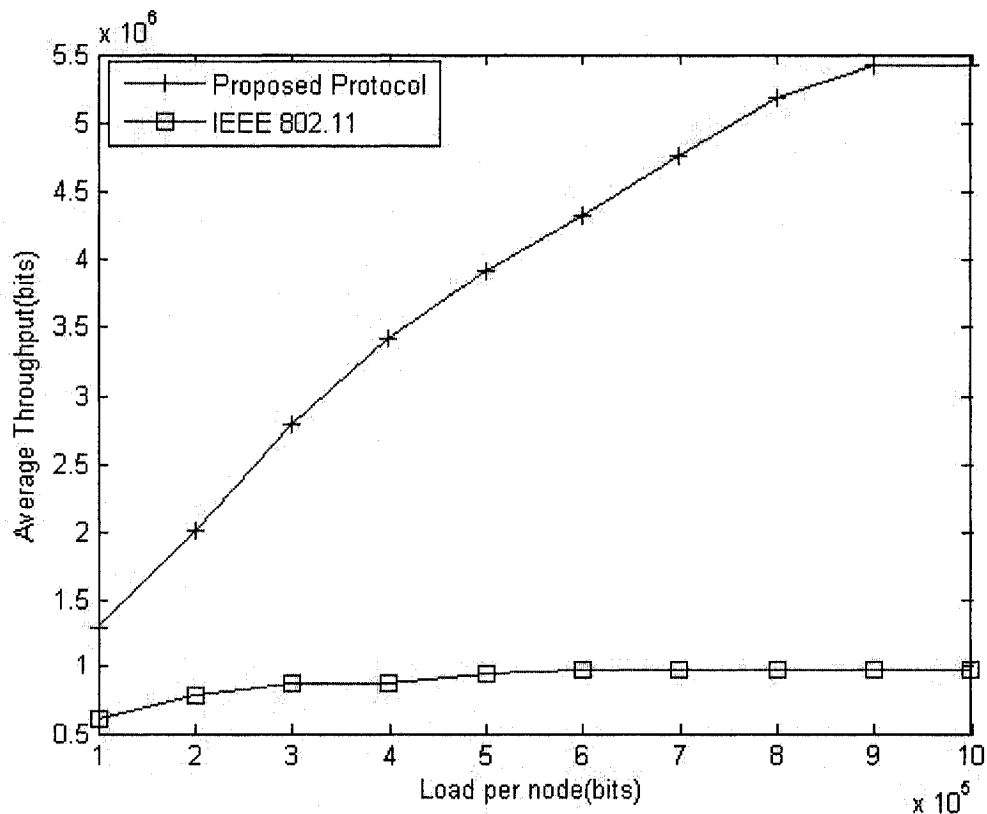


**Figure 5.7 Average throughput in AWGN channel (30 mobile nodes and 30 random topologies), SNR = 20dB, NOE = 6 (not applied to IEEE 802.11).**

## **5.4 Summary**

The simulation results presented throughout this chapter show how our system throughput is affected by different parameters such as SNR, NOEs, mobile node density, average load per node, and channel type. In particular, all the results presented clearly indicate how our proposed protocol outperforms the IEEE 802.11 protocol under different operating scenarios.

# Chapter 6

## Conclusions and Future Work

### *6.1 Conclusions*

In this thesis, we investigated the performance of a modified 2-channel 2-mode MAC protocol presented earlier in the literature for ad hoc networks using adaptive antennas. The main contribution of this thesis can be summarized as follow:

1) The proposed protocol avoids the deafness and hidden terminal problems which can be solved by combining the use of two channels and two modes. These kinds of problems may cause unpredictable interference in the wireless ad hoc networks.

2) DOA estimation process solves the position dependence which requires all or part of mobile nodes positions to be known prior to the start of the transmission. Since the proposed protocol does not rely on any kind of location awareness equipments (e.g. GPS), it can be used in indoor environment where the position information cannot be provided or the accuracy cannot be promised.

3) Different from most of DMAC protocols introduced in the literatures, we investigated the performance of proposed protocol over fading channels. As shown from

our simulations, the advantage of the directional antenna is fully utilized by the new protocol, especially in multipath fading channels.

Simulation results have clearly demonstrated that our proposed protocol, compared with the IEEE 802.11, can use the channel more efficiently under the same channel parameters. Although the proposed protocol requires more bandwidth (two channels), the simulation results presented still give us a clear demonstration of the improvement achieved.

## **6.2 Future Works**

Throughout our performance evaluations, we used a ULA antenna. It is interesting to investigate any potential improvement in the system throughput that can be achieved by using different types of antenna arrays, for example a planer antenna or circular array.

The DOA estimation algorithms also require further investigation. In particular, one need to consider some practical solutions to overcome the large estimation errors associated with DOA in the neighborhood of 0 and 180 degrees.

We used two channels in our protocol to deal with the deafness and hidden terminal problem of adaptive antennas. Due to the large gap of the frame length between the DATA frame and control frames, channel one (omni-mode) is idle in most of the simulation time. This is because DATA frames only occupy channel two (direction-mode). Using the concept of multichannel [6], we can design a multichannel system with one omni-mode channel and several direction-mode channels to utilize the bandwidth more efficiently.

## **References**

- [1] E. M. Royer, "A Review of Current Routing Protocols for Ad Hoc Mobile Wireless Networks," IEEE Personal Communications, Apr. 1999.
  
- [2] S. Xu and T. Saadawi, "Does the IEEE 802.11 MAC Protocol Work well in Multihop Wireless Ad Hoc Networks?," IEEE Communications Magazine, Vol. 39, No. 6, pp130-137, Jun. 2001.
  
- [3] P. H. Lehne and M. Pettersen, "An overview of smart antenna technology for mobile communication systems," IEEE Communications Surveys, Nov.-Dec. 1999.
  
- [4] IEEE P802.11a, Draft Supplement to Standard for Information Technology – Telecommunications and information exchange between systems – Local and metropolitan area networks – Specific Requirements – Part II: Wireless LAN Medium Access control (MAC) and Physical Layer (PHY) Specifications: High Speed Physical Layer in the 5GHz Band, Jul. 1999.
  
- [5] ANSI/IEEE Std 802.11, Part 11: Wireless LAN Medium Access Control (MAC) and Physical Layer (PHY) Specifications, 1999 Edition.  
(see: <http://standards.ieee.org/getieee802/802.11.html>)
  
- [6] N. Jain, S. R. Das, and A. Nasipuri, "A Multichannel CSMA MAC Protocol with Receiver-Based Channel Selection for Multihop Wireless Networks," Communications and Networks. Tenth International Conference, Oct. 2001.

- [7] T. Kobayashi, "TCP Performance over IEEE 802.11 Based Multichannel MAC Protocol for Mobile Ad Hoc Networks," IEICE Trans. Vol. E86-B, No.4, Apr. 2003.
- [8] S. L. Wu, Y. C. Tseng, C. Y. Lin and J. P. Sheu, "A Multi-channel MAC Protocol with Power control for Multi-hop Mobile Ad Hoc Networks," The computer Journal, Vol. 45, No.1, 2002.
- [9] S. L. Wu, Y. C. Tseng and J. P. Sheu, "Intelligent Medium Access for Mobile Ad Hoc Networks with Busy Tones and Power Control," IEEE Journal on Selected Areas in Communications, Vol. 18, No.9, Sep. 2000.
- [10] Y. X. Pan, W. Hamouda and A. Elhakeem, "An Efficient Medium Access Control Protocol for Mobile Ad Hoc Networks Using Antenna Arrays," to appear in IEEE Canadian Journal of Electrical and Computer Engineering (CJECE).
- [11] R. R. Choudhury, X. Yang, R. Ramanathan and N. H. Vaidya, "Using Directional Antennas for Medium Access Control in Ad Hoc Networks," International Conference on Mobile Computing and Networking, Sep. 2002.
- [12] K. Nagashima, M. Takata, and T. Watanabe, "Evaluations of A Directional MAC Protocol for Ad Hoc Networks," Distributed Computing Systems Workshops, 24th International Conference, pp23-24, Mar. 2004.
- [13] M. Takata, K. Nagashima and T. Watanabe, "A Dual Access Mode MAC Protocol for Ad Hoc networks Using smart Antennas," IEEE International Conference, Vol. 7, pp20-24, Jun. 2004.
- [14] Y. B. Ko, V. Shankarkumar and N. H. Vaidya, "Medium Access Control Protocols using Directional Antennas in Ad Hoc Network," IEEE Computer and Communications Societies, Proceedings, IEEE, Vol. 1, pp26-30, Mar. 2000.

- [15] W. T. Chen, M. S. Pan, "An Adaptive MAC Protocol for Wireless Ad hoc Networks Using Smart Antenna System," Vehicular Technology Conference, IEEE 58<sup>th</sup>, VTC fall, 2003.
- [16] T. Ueda, S. Tanaka, D. Saha, S. Roy and S. Bandyopadhyay, "An efficient MAC protocol with direction finding scheme in wireless ad hoc network using directional antenna," Radio and Wireless Conference (RAWCON), 2003.
- [17] A. Nasipuri, S. Ye, J. You and R. E. Hiromoto, "A MAC protocol for mobile ad hoc networks using directional antennas," IEEE Wireless Communications and Networking Conference (WCNC), 2000.
- [18] R. Ramanathan, "On the Performance of Ad Hoc Networks with Beamforming Antennas," ACM MobiHoc, Oct. 2001.
- [19] IEEE 802.11 WIRELESS LOCAL AREA NETWORKS - The Working Group for WLAN Standards (see: <http://grouper.ieee.org/groups/802/11/>).
- [20] R. Schmidt, "Multiple Emitter Location and Signal Parameter Estimation," IEEE Transactions on Antennas and Propagation, Vol. AP-34(3), pp276-280, 1986.
- [21] D. Rao and K. V. S. Hari, "Performance Analysis of Root-MUSIC," IEEE Trans. Signal Processing 28, pp25-42, 1999.
- [22] A. Paulraj, R. Roy and T. Kailath, "A Subspace Rotation Approach to Signal Parameter Estimation," Proceedings of the IEEE, pp1044-1045, 1986.
- [23] R. Roy and T. Kailath, "ESPRIT-Estimation of Signal Parameters Via Rotational Invariance Techniques," IEEE Transactions on Acoustics, Speech, and Signal Processing, Vol. ASSP-37(7), pp984-995, 1989.

- [24] M. Haardt, and J. A. Nossek, "Unitary ESPRIT: How to obtain increase spatial smoothing technique for bearing estimation in a multipath environment," IEEE Trans. ASSP, Vol. 43, pp1232-1242, May. 1995.
- [25] T. S. Rappaport, "Indoor Radio Communications for Factories of the Future," IEEE Commun. Mag., Vol. 27, pp15-24, May. 1989.
- [26] S. Haykin, "Introduction to Adaptive Filters," Macmillan Publishing Company, New York, 1985.
- [27] B. Widrow and M. E. Hoff, "Adaptive Switch Circuits," Part 4, IRE WESCOM, 1960.
- [28] B. D. Van Veen and K. M. Buckley, "Beamforming: A Versatile Approach to Spatial Filtering," IEEE ASSP Magazine, Apr. 1998.
- [29] B. Widrow and S. D. Stearns, "Adaptive Signal Processing," Prentice Hall, Englewood Cliff, NJ, 1985.
- [30] B. Widrow and P. E. Mantey, L. J. Griffiths, and B. B. Goode, "Adaptive antenna systems," Proc IEEE, pp2143-2159, Dec. 1967.
- [31] H. Arslan and E. Gregory. Bottomley, "Channel estimation in narrowband wireless communication systems," John Wiley, Wireless Communication and Mobile Computing, Vol. 1, Issue 2, pp201-219, 2001.
- [32] D. N. Goddard, "Self-Recovering Equalization and Carrier Tracking in a Two Dimensional Data Communication System," IEEE Trans. Comm., Vol. 28, pp1867-1875, 1980.

- [33] A. F. Naguib, "Adaptive Antennas for CDMA Wireless Networks" Ph.D. dissertation, Stanford University, Aug. 1996.
- [34] B. Sklar, "Rayleigh fading channel in mobile digital communication systems," Communication Magazine, IEEE, Vol. 35, Issue 9, Sep. 1997.
- [35] C. Tepedelenlioglu and A. Abdi, "The Ricean K factor: estimation and performance analysis," Wireless Communications, IEEE Transaction, Vol.2, Issue 4, pp799-810, Jul. 2003.
- [36] J. R. Treichler and B. G. Agee, "A New Approach to Multipath Correction of Constant Modulus Signals," IEEE Trans. Acoustic, Speech, and Signal Processing, Vol. ASSP-31, pp459-472, Apr. 1983.
- [37] A. Michalski and J. Czajewski, "The Accuracy of the Global Positioning Systems," IEEE Instrumentation and Measurement Magazine, Mar. 2004.
- [38] B. Agee, "Blind Separation and Capture of Communication Signals Using a Multitarget Constant Modulus Beamformer," IEEE Military Communications Conference, pp340-346, 1989.
- [39] T. Biedka, Virginia Tech Adaptive Array Seminar, 1997.
- [40] Alberto Leon-Garcia, Indra Widjaja, "Communication Networks Fundamental Concept and Key Architectures," Second Edition, Mc Graw Hill, 2003.
- [41] J. Liberty, Theodore S. Rappaport, "Smart Antenna for wireless Communications," Upper Saddle River, NJ:Prentice Hall, 2000.

- [42] B. Noble, "Methods Based on the Wiener-Hopf Technique for the solution of partial differential equations," Pergamon Press, London, 1958.
- [43] Alberto Leon-Garcia, "Probability and Random Processes for Electrical Engineering," Second Edition, Addison Wesley, 1994.
- [44] N. Patwari and Joshua N. Ash, "Locating the Nodes," IEEE Signal Processing Magazine, pp54-69, Jul.2005.
- [45] B. Xu and S. Hischke, "The role of Ad hoc Networking in Future Wireless Communications," Communication Technology Proceedings, ICCT, 2003.
- [46] Y. Ko and V. Shankarkumar, "Media Access Control Protocols Using Directional Antennas in Ad hoc Networks," IEEE INFOCOM, 2000.
- [47] B. Sklar, "Digital Communications -- Fundamental and Applications," Second Edition. Upper Saddle River, New Jersey, 2001
- [48] C. A. Balanis, "Antenna Theory: analysis and design," Second Edition. Hoboken NJ, John Wiley, 1997.